CHALMERS

Robustness and Reliability of Front Underrun Protection Systems

Master's Thesis in Solid and Fluid Mechanics

JOHANNES FRÄMBY
DAVID LANTZ

Department of Applied Mechanics
Division of Dynamics
CHALMERS UNIVERSITY OF TECHNOLOGY
Göteborg, Sweden 2010
Master's Thesis 2010:62

MASTER'S THESIS 2010:62

Robustness and Reliability of Front Underrun Protection Systems

Master's Thesis in Solid and Fluid Mechanics

JOHANNES FRÄMBY
DAVID LANTZ

Department of Applied Mechanics
Division of Dynamics
CHALMERS UNIVERSITY OF TECHNOLOGY
Göteborg, Sweden 2010

Robustness and Reliability of Front Underrun Protection Systems
JOHANNES FRÄMBY
DAVID LANTZ

Master's Thesis 2010:62
ISSN 1652-8557
Department of Applied Mechanics
Division of Dynamics
Chalmers University of Technology
SE-412 96 Göteborg
Sweden
Telephone: + 46 (0)31-772 1000

Cover:
Collision between passenger car and heavy goods vehicle. ©Lars Forsman.

Chalmers Reproservice
Göteborg, Sweden 2010

Robustness and Reliability of Front Underrun Protection Systems
Master's Thesis in Solid and Fluid Mechanics
JOHANNES FRÄMBY
DAVID LANTZ
Department of Applied Mechanics
Division of Dynamics
Chalmers University of Technology

Abstract

In 2001, the United Nations Economic Commission for Europe decided that all trucks manufactured as from that year need a *front underrun protection system* (FUPS). This as a step in order to decrease fatalities in head-on collisions between *heavy goods vehicles* (HGV) and passenger cars. A further development of the FUPS is an *energy absorbing* FUPS (EA-FUPS). For a safety system like the EA-FUPS it is important that its functions work properly in both expected and unexpected crash scenarios. In other words, the system should be robust. In addition to a robust behaviour one would like to determine the successfulness of the system, *i.e.*, the reliability of the system should be evaluated.

This Master's Thesis contains a reliability and robustness study of an EA-FUPS, where stochastic analysis of a head-on collision between an HGV and a passenger car has been utilised. In this analysis the *probability density functions* (PDF:s) of collisions and structural parameters have been set up according to statistics from real-world accidents and manufacturing data. Several responses from the numerous crash simulations, solved with an explicit finite element method, were logged and statistics were used to set up, *e.g.*, probabilities and scatter plots to evaluate the system.

The results show a FUPS that, although the energy absorbing capabilities are rather non-robust and unreliable, fulfills its prime objective, which is protecting the passenger car from underrunning the HGV. However, when the vehicle overlap is small the FUPS is not stiff enough to protect the wheel from being hit. There are several reasons for the unreliable energy absorption level, *e.g.*, the energy absorbing mechanism has poor compatibility with the front structure of many passenger cars. Besides the resulting reliability and robustness analyses, an algorithm for performing robust CAE is presented.

Keywords: Front underrun protection, robust FUP, FUPD, FUPS, EA-FUPS, UN ECE-R93, FEA, stochastic analysis

Contents

Preface

This report covers the Master's Thesis on a robustness and reliability study of Front Underrun Protection Systems (FUPS), [1]. The Master's Thesis was performed during 2010 at Epsilon Utvecklingscentrum Väst AB in collaboration with Volvo Trucks and the Department of Applied Mechanics at Chalmers University of Technology.

We would like to thank our supervisors, Johan Iraeus and Dag Tuvesson, Epsilon, examiner, Mikael Enelund, the Department of Applied Mechanics at Chalmers University of Technology and Volvo Trucks for their support and expertise throughout the thesis.

Göteborg November 2010
Johannes Främby, David Lantz

Abbreviations

ANSA	Commonly used commercial pre-processing software
CAE	Computer-aided engineering
CDF	Cumulative distribution function
CI	Confidence interval
COD	Coefficient of determination
c_v	Coefficient of variation
EA-FUPS	Energy-absorbing front underrun protection system
FEA	Finite element analysis
FUPS	Front underrun protection system
LHS	Latin Hypercube sampling
LS-DYNA	General purpose finite element package
LS-OPT	Optimization tool, also suitable for stochastic analysis
MCS	Monte Carlo simulation
PDF	Probability density function
RADIOSS	General purpose finite element package
UN ECE	United Nations Economic Commission for Europe

1 Introduction

In statistical data provided by the Swedish Transport Administration (formerly known as Vägverket) [1] and the German insurance institute for traffic engineering (GDV) [2] a large part of head-on collisions between passenger cars and *heavy goods vehicles* (HGV:s) end up with fatalities in the car. Besides structural differences the main reason is the large difference in kinetic energy and momentum between the passenger car, referred to as car, and the HGV, referred to as truck. This is a problem on single carriageways, which are very common in, *e.g.*, Northern and Eastern Europe and Great Britain.

According to current regulations UN ECE-R93[i] [3], trucks manufactured after 2001 [4] must be equipped with an underrun protection in the front, a so called *front underrun protection system* (FUPS). This must in a head-on collision with a car stop the car from going under the truck and at the same time engage the crash protection of the car with its energy-absorbing front structure. The present certification requirements on a FUPS are partly a geometric demand to meet the structure of the car and a static force level that the FUPS must withstand in order to satisfy the above functionality.

Today's FUP-systems usually consist of a transverse horizontal beam (FUP-beam), whose position is regulated by UN ECE-R93, rigidly attached to the longitudinal main chassis of the truck, see Figure 1.1. A further development of this is an *energy-absorbing FUPS* (EA-FUPS) where the FUP-beam is allowed to move backward up to a limiting depth and at the same time absorb energy. This allows the truck to absorb some of the kinetic energy in a collision, meaning that less damage will be subjected to the car [1].

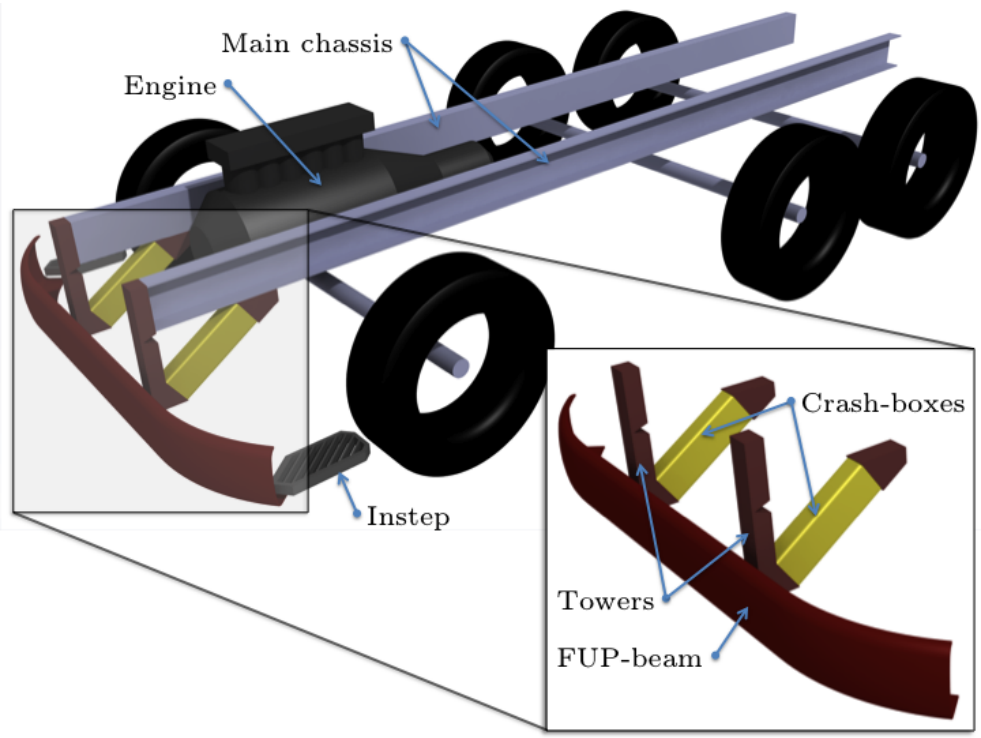

Figure 1.1: The main structure of a truck with the EA-FUPS in close up.

[i]European Commission directive regulating the deformation of the front underrun protection device when applying static loads according to UN ECE-R93.

1.1 Purpose

For a safety system, like the FUPS, to have maximum protective effect its functions need to work properly in both expected and unexpected crash scenarios thus covering a wide range of the most accident scenarios. This can be interpreted as that the system should be robust [5]. What criteria to be used when describing the robustness of a FUPS are, however, not obvious.

Today there is no test or simulation method for this purpose and in addition to certification testing, only limited evaluation is performed. The development of energy absorbing FUP-systems would require a better understanding and a qualitative measurement of the robustness, such that new systems can be evaluated properly. In long term, certification testing should be evolved to evaluate the energy absorbing abilities, but in the mean time systems like this need to be properly evaluated during development. This is where robust CAE analysis can contribute.

1.2 Scope

The project scope is to take an existing finite element model of a car and a truck, equipped with an EA-FUPS, and simulate the collision stochastically according to a predefined load space based on statical data from real accidents. From the results, robustness and reliability analyses of the FUPS shall be presented in addition to suggestions on design modifications to improve the robustness. The methodology presented and used to analyse the system is supposed to be applicable on other FUPS, however, in this thesis only the Volvo FUPS is analysed.

1.3 Overview of method

As stated above the purpose of a robustness analysis is to find the response from a wide range of expected and unexpected loading scenarios. When the response shows high degree of predictability the robustness can be deemed high while the opposite can be said if the system response is unpredictable.

To perform a robustness analysis, parametric studies (deterministic analysis) can be conducted, however, in this project stochastic analysis has been used. This basically means that instead of using only nominal values (plate thickness, material data, impact angles, speeds, *etc.*) partly random combinations of the input parameters are used. The reason for this type of analysis, with stochastic simulations, is that the robustness of a system like FUPS can not be determined easily with parametric studies [5].

The results from the stochastic analysis can then be used to analyse the total performance of the system by different means. If the goal is to simply evaluate the robustness or reliability the results will, besides presenting the performance under different loading cases, also give information about the probability of certain responses (this demands input parameters that represent real working conditions). Since no system is perfect, knowledge about the likelihood of failure can be invaluable. When the purpose of the analysis is improvement, the results can be processed by, *e.g.*, *principal component analysis* (PCA), which finds the response with dominating variability and the system can be altered in a way that affects the robustness the most [5].

2 Theory

This chapter describes the basics of a number of tools needed in this thesis. The first section concern mathematical statistics and probability. The subsequent section gives a view of how stochastic analysis is performed. The last section in this chapter introduces the finite element method.

2.1 Statistic analysis

In this section some definitions in mathematical statistics and probability and a brief overview of the analysis tools for handling statistic data used in the thesis will be given. For further reading see textbooks on the topic, *e.g.*, [6]. The text below is taken mainly from [6] and [7].

The probability P is defined as a positive measure, between 0 and 1, associated with an event in probability space. When the event is defined as the occurrence of a real random value X, being smaller than a prescribed value x, this is called the *cumulative distribution function* (CDF):

$$F_X(x) = P[X < x] \tag{2.1}$$

which can be differentiated with respect to x to yield the *probability density function* (PDF):

$$f_X(x) = \frac{\mathrm{d}}{\mathrm{d}x} F_X(x). \tag{2.2}$$

There are different ways to describe a random variable X, most common are the *expected value* $\mathbf{E}[X]$ and the *variance* $\mathrm{var}[X]$. The expected value, which can be interpreted as the long run average value, is often approximated as the *mean value* $\overline{X}$ (*N.B.:* this must not be the most probable sample value). The variance is a measure of the distance the sample values x has to the mean value. In Equation 2.3 and 2.4 the expected value and variance are defined for a continuous PDF.

$$\mathbf{E}[X] = \mu_X = \int_{-\infty}^{\infty} x f_X(x) \mathrm{d}x \tag{2.3}$$

$$\mathrm{var}[X] = \sigma_X^2 = \mathbf{E}[(X - \mu_X)^2] = \int_{-\infty}^{\infty} (x - \mu_X)^2 f_X(x) \mathrm{d}x \tag{2.4}$$

The positive square root of the variance is called the *standard deviation* σ_X and is often used to describe the dispersion of the distribution of X. It is also used in the *coefficient of variation* c_v (for a non-zero mean):

$$c_v = \frac{\sigma_X}{\mu_X}. \tag{2.5}$$

2.1.1 Data description

The mean and variance for the samples $x_i, i = 1, 2, ..., N$, are often approximated as the *sample mean* $\overline{x}$ and *sample variance* s^2, defined as

$$\overline{x} = \frac{1}{N} \sum_{i=1}^{N} x_i \tag{2.6}$$

and

$$s^2 = \frac{1}{N-1} \sum_{i=1}^{N} (x_i - \overline{x})^2 \tag{2.7}$$

respectively, see [6].

The *median* m in N samples is defined as the the value at position $\frac{1}{2}N$, when these have been sorted in increasing order.

One way of describing the distribution of the samples $x_i, i = 1, 2, ..., N$, is the *five finger summary* (FFS), which involves the median, the *first* and *third quartile* (Q_1 and Q_3), *lower* and *upper* acceptable extremes (L and U), as (L, Q_1, m, Q_3, U). Q_1 is the observation at $(\frac{1}{4}N + \frac{1}{2})$-th place and Q_3 is the observation at $(\frac{3}{4}N + \frac{1}{2})$-th place in the increasingly ordered sample. Upper and lower extremed are defined as:

$$L = \min \begin{bmatrix} \min[x_i] \\ \text{and} \\ Q_1 - 1.5(IQR) \end{bmatrix} \tag{2.8}$$

and

$$U = \max \begin{bmatrix} \max[x_i] \\ \text{and} \\ Q_3 + 1.5(IQR) \end{bmatrix} \tag{2.9}$$

where

$$(IQR) = Q_3 - Q_1 \tag{2.10}$$

is the *inter-quartile range*. In Figure 2.1 a FFS is represented by a *boxplot* (also called *box-and-whisker plot*).

When describing the distribution of samples one can set up a *confidence interval* (CI) for which there is a probability of 1 - α of picking a sample x_k contained within interval [L,U] such that

$$P[L \leq x_k \leq U] = 1 - \alpha \tag{2.11}$$

where $0 \leq \alpha \leq 1$, see Figure 2.2 for an example. If a confidence level α is set (often to 0.01 or 0.05) for a specific sample distribution the corresponding CI will be given. The CI is used to verify how well the estimate to the statistics describe the distribution, *e.g.*, on the sample mean or on the probability of succeeding a specified system performance.

Besides the distribution descriptions above, two other measurements can be useful in a robustness analysis, *i.e.*, *skewness* and *kurtosis*, see [5].

Skewness, also called the third standardized moment, is a measure of the degree of symmetry in a distribution. The *sample skewness* g_1, defined in Equation 2.12, is equal to zero in a symmetric distribution, negative when the left tail is longer than the right and

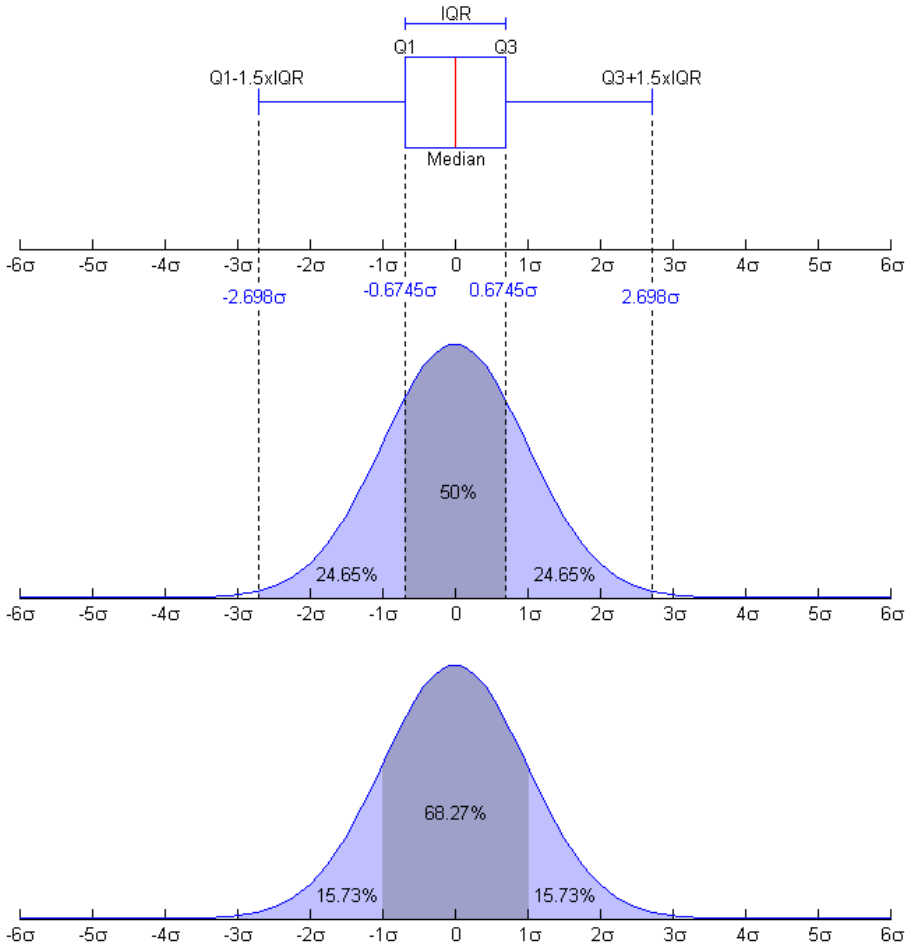

Figure 2.1: Boxplot (top) with the corresponding sample fraction of each part in the Normal $N(0, \sigma^2)$ population (middle) compared to the fractions of the standard deviation σ (bottom).

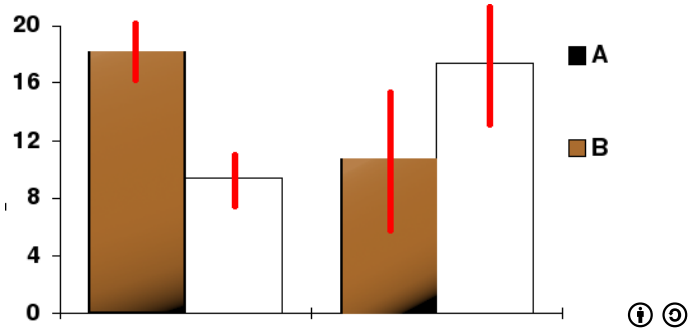

Figure 2.2: Examples of confidence intervals (in red) on estimations visualised as bar charts.

the main part of the mass is concentrated on the right hand side while positive skewness shows the opposite, see Figure 2.3.

$$g_1 = \frac{1}{N-1}\sum_{i=1}^{N}\left(\frac{x_i - \overline{x}}{s}\right)^3 \tag{2.12}$$

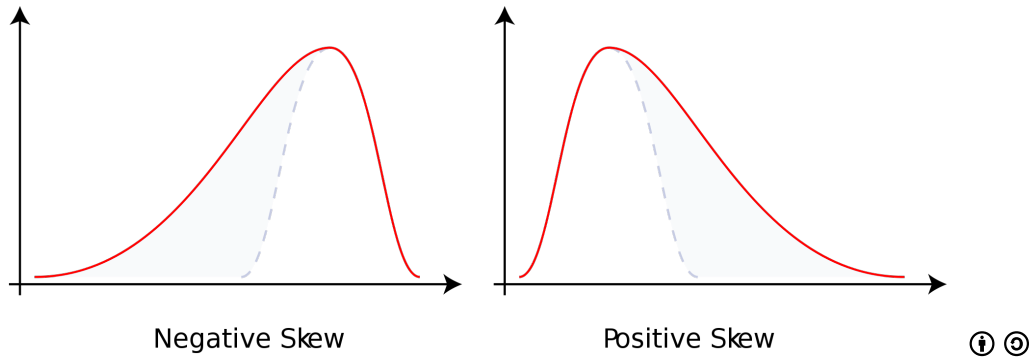

Figure 2.3: Examples of distributions with negative and positive skewness.

Kurtosis, or the fourth standardised moment, is a measure of the peakedness or weight of the tails of a distribution. High kurtosis describes a distribution with long thin tails and a high peak indicating that the variance is a result of infrequent extreme deviations as opposed to frequent deviations in low kurtosis. In Equation 2.13 below, the *excess sample kurtosis* g_2 is defined, where the "minus 3" is present to make the (excess) kurtosis of the standard normal distribution equal to zero (see Section 2.1.2 for probability distributions).

$$g_2 = \frac{1}{N-1}\sum_{i=1}^{N}\left(\frac{x_i - \overline{x}}{s}\right)^4 - 3 \tag{2.13}$$

In this way the kurtosis can be related to how similar it is to the normal distribution. In Figure 2.4 the excess kurtosis for different distributions are plotted.

When a system handles multivariate statics, *i.e.*, a large number of random variables, $X_1, X_2, ..., X_N$ occur together, the variables can be collected in a *random vector* $\mathbf{X}$ as

$$\mathbf{X} = [X_1, X_2, ..., X_N]^T \tag{2.14}$$

and be inserted in the definitions for mean, variance, skewness and kurtosis above to create the corresponding vectorial entities of these.

2.1.2 Probability density functions

Some continuous PDF:s have been analytically defined and the most frequent ones are described below, however, several others exist and can be found in textbooks like [6].

The simplest PDF is the *continuous uniform distribution* $U(a, b)$, which has the same probability in the interval [a,b] as defined in Equation 2.15. An example with the interval [-1.7,1.7] can be seen in Figure 2.4.

$$f(x) = \begin{cases} \frac{1}{b-a} & \text{for } a \leq x \leq b \\ 0 & \text{else} \end{cases} \tag{2.15}$$

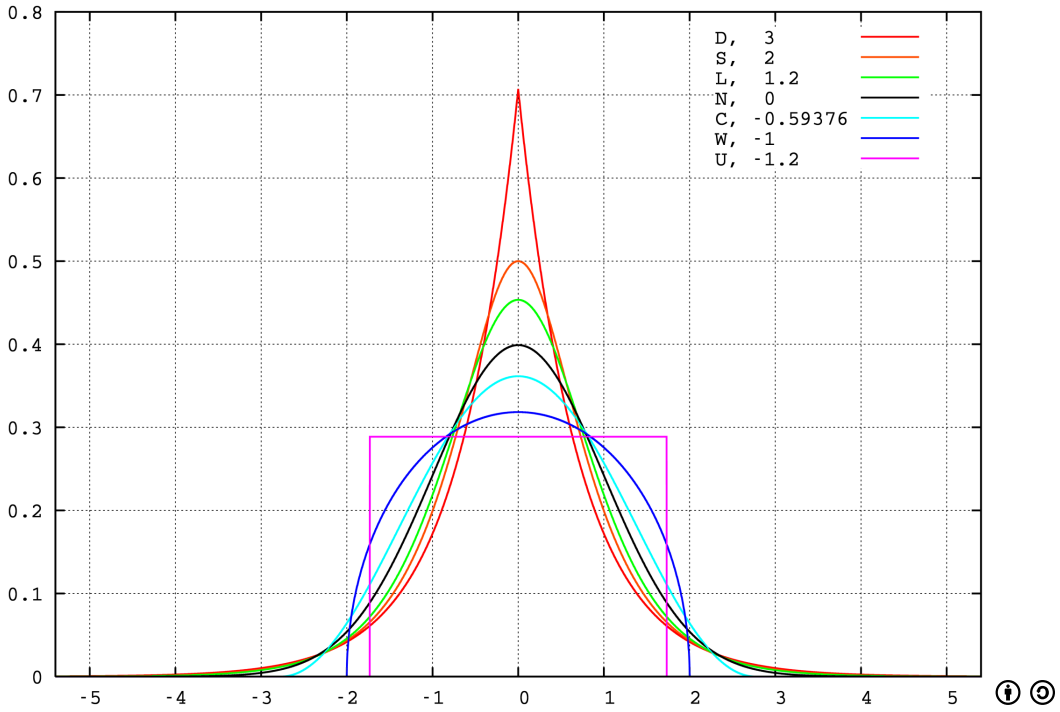

Figure 2.4: Example of excess kurtosis for the Laplace (D), hyperbolic secant (S), logistic (L), normal (N), raised cosine (C), Wigner semicircle (W) and uniform (U) distributions.

Undoubtedly the most widely used PDF-model is the *normal distribution* $N(\mu, \sigma)$, also called *Gaussian distribution*. This is because of natural phenomena tend to show a normal distribution when the sampling size becomes large. The distribution was developed by De Moivre in the *central limit theorem*, in 1733, however, because of unfortunate events, his work was lost and Gauss independently developed the normal distribution nearly 100 years later. The normal PDF is defined in Equation 2.16 and examples of normal PDF:s and the integrated CDF:s can be seen in Figure 2.5. A normal random variable with zero mean and a standard deviation of 1 is called a *standard* normal random variable with distribution $N(0, 1)$ [6].

$$f(x) = \frac{1}{\sqrt{2\pi\sigma^2}} \exp^{-\frac{(x-\mu)^2}{2\sigma^2}} \tag{2.16}$$

2.1.3 Regression analysis

In multivariate statistics, a *regression analysis* focuses on the relationship between dependent (response) variables and the independent (input) variables. The goal is a *regression model* (also called *meta-model* or *surrogate model*) where an estimate $\hat{\mathbf{Y}}$ to the expected value of the responses $\mathbf{Y}$ are functions of the independent variables $\mathbf{X}$ and the parameters $\boldsymbol{\beta}$ as seen in Equation 2.17. The purpose of the regressions are to minimize the error terms $\boldsymbol{\epsilon}$. To perform a regression analysis the functions must first be chosen, for example, in the linear regression in Equation 2.18 there is a linear relationship between the response variable and multiples of the independent variables, see Figure 2.6.

$$\mathbf{Y} = \hat{\mathbf{Y}} + \boldsymbol{\epsilon} = \mathbf{f}(\mathbf{X}, \boldsymbol{\beta}) + \boldsymbol{\epsilon} \tag{2.17}$$

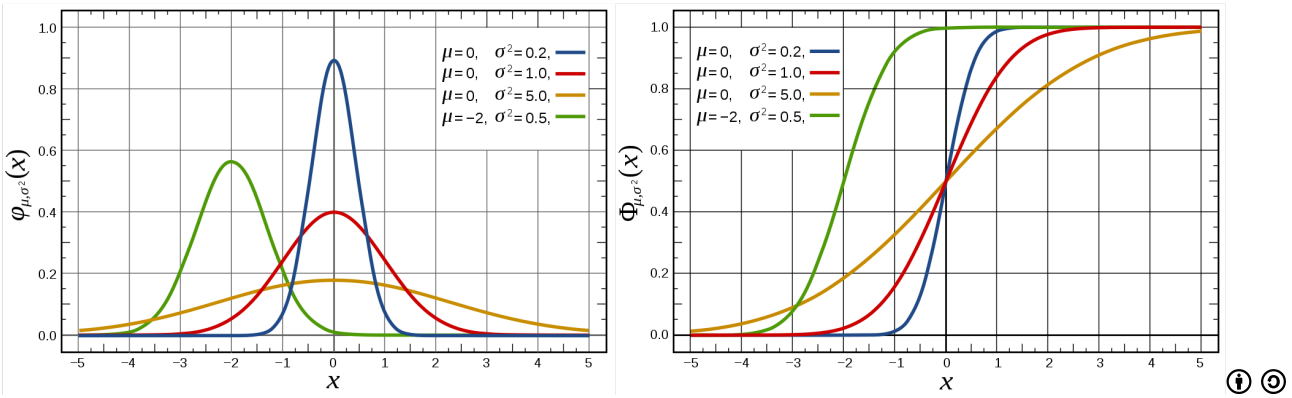

Figure 2.5: Examples of probability density function (a) and cumulative density functions (b) of the normal distribution.

$$\mathbf{Y} = \sum_{k=1}^{N} \boldsymbol{\beta}_k \mathbf{X}^k + \boldsymbol{\epsilon} \tag{2.18}$$

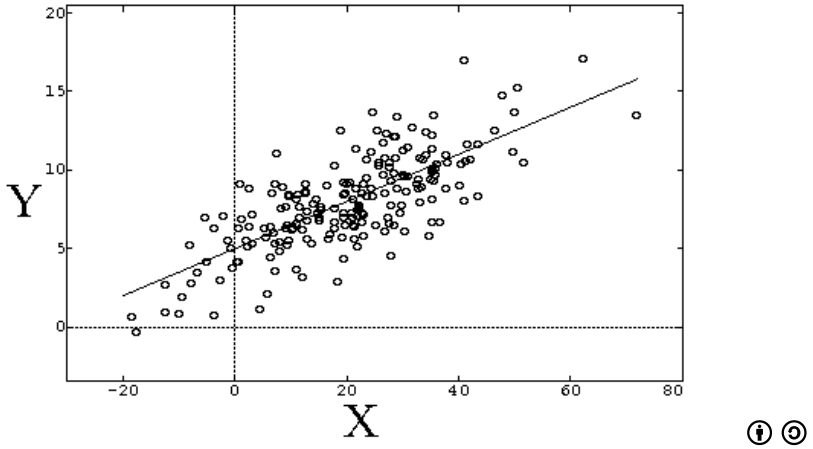

Figure 2.6: Example of linear regression for several sets of responses $\mathbf{Y}$ and independent variables $\mathbf{X}$.

2.1.4 Association between variables

Different associations between the variables in a random vector $\mathbf{X}$ can be defined to show couplings and dependencies in a system. Below, some different associations relevant for this thesis are defined.

For two sets of random vectors $\mathbf{X}$ and $\mathbf{Y}$ the *covariance matrix* describes how much the random entities in $\mathbf{X}$ change together with those in $\mathbf{Y}$. This is defined as

$$\mathbf{C_{XY}} = \mathbf{E}[(\mathbf{X} - \boldsymbol{\mu}_\mathbf{X})(\mathbf{Y} - \boldsymbol{\mu}_\mathbf{Y})^T], \tag{2.19}$$

where the matrix entities can be divided with the product of the respective standard deviations to create the dimensionless *coefficient of correlation*, also called *Pearson correlation coefficient*:

$$\rho_{ij} = \frac{\mathbf{E}[(X_i - \mu_{X,i})(Y_j - \mu_{Y,j})]}{\sigma_{X,i}\sigma_{X,j}}. \tag{2.20}$$

The correlation gives the first-order dependency between two random variables, but unlike the covariance it becomes limited to the interval [-1,1]. A positive or negative correlation describes a total positive or negative linear relation respectively while independency between the variables yields a zero value. However, the inverse is not true; a zero value does not ensure independency, since the correlation cannot find higher order dependencies, see Figure 2.7 for examples. The correlation has an equivalent sample version where the factors in Equation 2.20 are replaced with the equivalent sample versions.

In order to find non-linear or other correlations between variables, another type of association must be used. An example is *rank*, which is a measure of how well the relationship between two variables can be described using a monotonic function, *i.e.*, if one variable increases and the other does too a high rank is given, see Figure 2.8. For definitions of rank, *e.g.*, *Spearman's* or *Kendall's*, see [6].

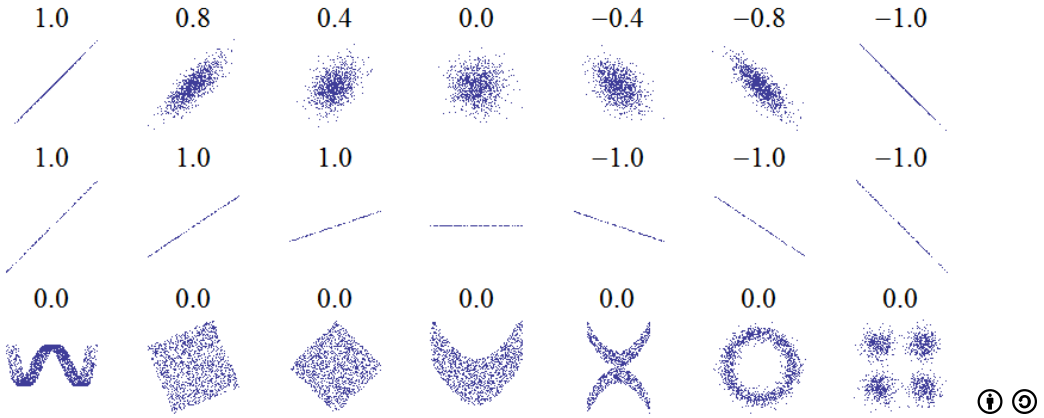

Figure 2.7: Examples of correlation values between two sets of points. Note that the correlation reflects the noisiness and direction of linear relationships but not the slope or any non-linear relationships. The center example shows independency between the variables, however, since the variance is zero for the points in the ordinate the correlation is undefined.

Besides the analysis tools already mentioned, several others can be defined to couple the input variables to output (response) variables (I/O) or the output to each other (O/O). One is the *coefficient of determination* (COD), which utilises the underlying regression model (such as, *e.g.*, linear or quadratic) to build an approximation to the experimental input-output relation. The COD can be used to give the relevance of the approximation by the regression model. The importance of one variable is then measured by the decrease of COD when removing this variable from the regression model [7].

The COD, which in [8] is defined as R_i^2, represent the percent of the response data y_i that is the closest to the regression model $\hat{y}(x_i)$. For example, if $R_i^2 = 0.8$ when based on a linear model, 80 % of the total variation of the response y_i can be explained by the linear relationship with the regression model $\hat{y}$ which is a function of x_i.

The *coefficient of importance* which is based on the COD is a prediction value to explain the influence of a single input parameter and the definition can be found in [8].

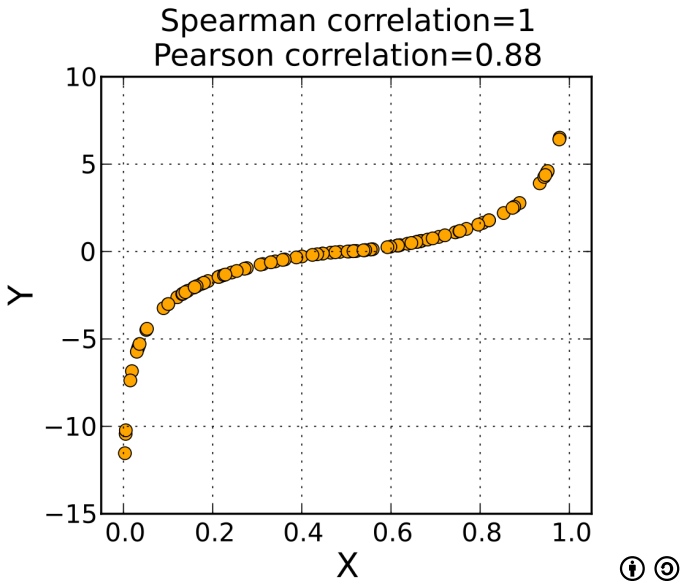

Figure 2.8: Example of different correlation values between two sets of points, while Spearman's rank captures the monotonic relation perfectly, Pearson's correlation does not.

2.2 Stochastic analysis

The main difference between deterministic and stochastic analyses is that while the first uses fixed input parameters to evaluate a system the latter has its base in the fact that most parameters in real world applications are random variables. When a product development process involves the improvement of a system the following uncertainties are present [7]:

- Design variables: Depending on level of quality in the manufacturing process, uncertainties in the design parameters may occur. The degree of influence on the response can be used to obtain information about tolerances and quality required in components.
- Objective function: In some applications the loading conditions and other external parameters affecting the system can be quite straightforward but in several others, *e.g.*, an automotive crash, the parameters controlling the crash are nearly impossible to foresee.
- Feasible domain: When a deterministic optimisation is run, the entire response domain is not spanned and the deterministic optimum might be in or close to the unfeasible domain. Such problems are at the core of probability-based simulations.

The stochastic analysis can also be part of a robustness analysis where the results are used to validate the system performance for the entire input domain. This is essentially the first step of an optimisation or improvement scheme where the goal is robustness. As most product development processes start with some sort of specification of demands, a reliability analysis can be a tool for validating these demands and give information about the risk of failure under working conditions.

2.2.1 Input parameters

The input parameters to a system analysis can be divided into the following categories:

- Design variables are variables that can be controlled and are the main tool to change the system's performance.

- Loading variables can to some extent be controlled depending on boundary conditions but in many cases these are hard to set constant with full confidence. Often the result of this is that the worst case scenario is tested instead of creating loading conditions that represent real working conditions thus leading to oversized and/or overcompensated system designs.

- Noise is a result of natural variations in system parameters and are often beyond control. These can have little or large effect on the system depending on application, *e.g.*, if the material data is considered, a polymer structure would have a larger spread in stiffness than most steel structures would.

To make a fair robustness analysis the input data should represent reality as close as possible; in the case of a FUPS analysis, these should rely on statistical data, which describes how real accidents occur. These input parameters, which define the loading of the system, should then be combined with the design parameters and noise. Collecting and generating an input space that represents true working conditions is an important step in the stochastic analysis which could cause a problem. Especially when the analysis is performed early in a product development process when a large quantity of the loading conditions are unknown. However, just spanning the input domain can give valuable information about its effect on the system performance.

The number of parameters to vary in a system can be almost infinite and a decision based on engineering reasoning may be necessary to choose the most important ones. This is not only a question of how complex the analysis will become but also of processing cost. Each variable added will require more analyses; a rule of thumb is that n variables require n^2 simulations to have the statistical properties of the response converged [9].

2.2.2 Analysis scheme

Depending on what kind of stochastic analysis to be done the simulation scheme can differ, however, since this project was a direct robustness analysis the *Monte Carlo simulation* (MCS) could be employed.

There is no single Monte Carlo method, instead it is a term describing a wide range of applications with similar approaches. It is a computational algorithm that rely on repeated random sampling to compute the results. Typical applications can be when there is high uncertainty in the input or when it is impossible to compute an exact result deterministically. As the name implies, the method refers to the famous casino in Monaco where randomness is used. From a population the Monte Carlo method selects a subset, which still represents the original distribution, and tries to approximate arbitrary probability distributions [10].

In this analysis a commercial optimisation software called LS-OPT [11], which has adopted the following MCS scheme, has been used:

1. Define a domain of possible input variables.

2. Repeat until convergence in statistical properties (*e.g.*, sample mean and variance) or the upper limit of number of allowed simulations is reached:

   (a) Select the random sample points from the input domain according to a user specified strategy and the statistical distributions assigned to the input variables.

   (b) Perform a deterministic simulation (in this project a head-on collision between a car and a truck) to calculate the system response.

3. Collect and evaluate the statistics of the responses.

In the sampling step, 2a, different methods can be applied to selecting the points. While random sampling (sometimes noted Monte Carlo sampling) is supposed to choose the points in a random or pseudorandom manner there are algorithms like *Latin Hypercube sampling* (LHS), which is an advanced Monte Carlo sampling. LHS is a sort of stratified random sampling where the input space is divided into layers and requires fewer sampling points to represent the design space compared to Monte Carlo [8]. The sampling from the layers is performed and different simulation sets, called hypercubes, are put together randomly or via an optimisation algorithm in order to generate a good multidimensional spreading [10].

2.2.3 Post-processing

After a simulation several post-processing algorithms can be utilised depending on the type of analysis. If reliability and robustness are to be evaluated the statistics of the response can be used to set up probability of succeeding the specified demands and PDF:s approximated on the response [11]. Analysis of the distribution of the response can also be deemed robust or non-robust with quantitative measurements as skewness or kurtosis as suggested by [5] (p. 139).

The response can also be used to build a regression model that can be interpolated and in some cases extrapolated to explore new designs. Surrogate models are well documented and for further reading on this topic see, *e.g.*, [5], [8] and [11].

When the variability of the system needs to be examined a *principle component analysis* (PCA) can be used to find the dominating variability. This combined with different correlation algorithms, *e.g.*, linear or higher order correlation, rank or coefficient of determination, can find the most important input parameters. Smith [12] contains a tutorial of PCA and in [5] (p. 126) one can find algorithms for including PCA in simulations schemes.

2.3 The finite element method

The finite element method (FEM) is a numerical procedure for solving partial differential equations widely used in engineering analysis of a physical problem. The physical problem, that can be both structures and continua, is idealised to a mathematical model that via certain required assumptions leads to differential equations governing the mathematical model. Since the finite element solution technique is a numerical procedure, the results are rarely exact. Errors are decreased by adding more equations, *i.e.*, creating finer mesh until sufficient accuracy is reached.

The finite element method originated as a method of stress analysis but is today also used in heat conduction, fluid flow, crash-analysis *etc.* It is used when problems become too complicated to solve with traditional analytical methods. The algebraic equations, produced by the finite element procedure, are generated and solved on digital computers. The complexity of the model describing the problem is therefore dependent on the performance of the computer [13], [14].

3 Method

This chapter is divided into description of the simulation model, input variables from statistical data and the analysis of the response. When developing an FE-model one must first choose a unit system and use it consistently through out the work. For this simulation a unit system common in crash simulation has been chosen, see Table 3.1.

Table 3.1: Unit system used troughout the thesis.

Length	Time	Mass	Force	Pressure	Velocity	Density	Energy
mm	ms	kg	kN	GPa	m/s	M kg/dm^3	J

3.1 Crash simulation

To be able to analyse the FUPS, simulation with some sort of software was needed and therefore a dynamic FEA was performed on the system. The first 120 ms of the crash was analysed since this proved to be sufficient to observe the effects on the FUPS. The materials were modeled as elasto-plastic[ii]. The FE-model used to simulate the crash between the truck and the car will be referred to as the simplified FE-model.

3.1.1 Simplified FE-model

In a robustness analysis it is of importance to perform enough simulations to get convergence in the statistical results. To be able to run the desired number of analyses in as short time period as possible the FE-model needs to be relatively small. This was the reason for making simplifications to an FE-model received from Volvo Trucks.

The FE-model used by Volvo Trucks to evaluate FUP-systems consists of a Volvo truck and a car. Since it was the FUPS of the truck being evaluated in this thesis the following simplifications were possible. The car was substituted to an FE-model of another car with a coarser mesh, having less than 30000 elements compared to 313000 elements in the original FE-model of the car. Because the FUPS is located in the lower front part of the truck it was possible to simplify parts of the truck that does not affect this area significantly in a head-on collision. Parts of the truck such as the engine, the front part of the longitudinal frame member and the leaf spring hanger, *cf.* Figure 3.1, were modeled as rigid bodies since these parts are larger and stiffer than the parts in the FUPS. The body and the parts behind the front axle of the truck were modeled as lumped masses and distributed in a way that the moment of inertia was comparable with the original. These simplifications reduced the size of the FE-model of the truck to 100000 deformable elements and thereby the computational cost significantly. A representation of the simplified FE-model of the truck can be seen in Figure 3.2.

The resulting FE-model called the simplified FE-model, consisting of the simplified truck and the simplified car, is presented in Figure 3.3. The total number of deformable elements in this simplified FE-model was 130000 elements compared to the original model that consisted of 1130000 deformable elements.

[ii]The deformation behaviour of an elaso-plastic material includes elastic and plastic deformation.

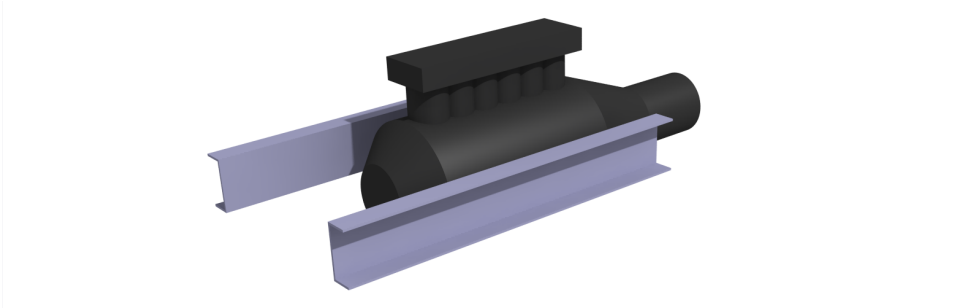

Figure 3.1: In the simplified truck FE-model the engine and the front chassis were modeled as rigid bodies with the remaining rear parts attached as lumped masses (not seen here).

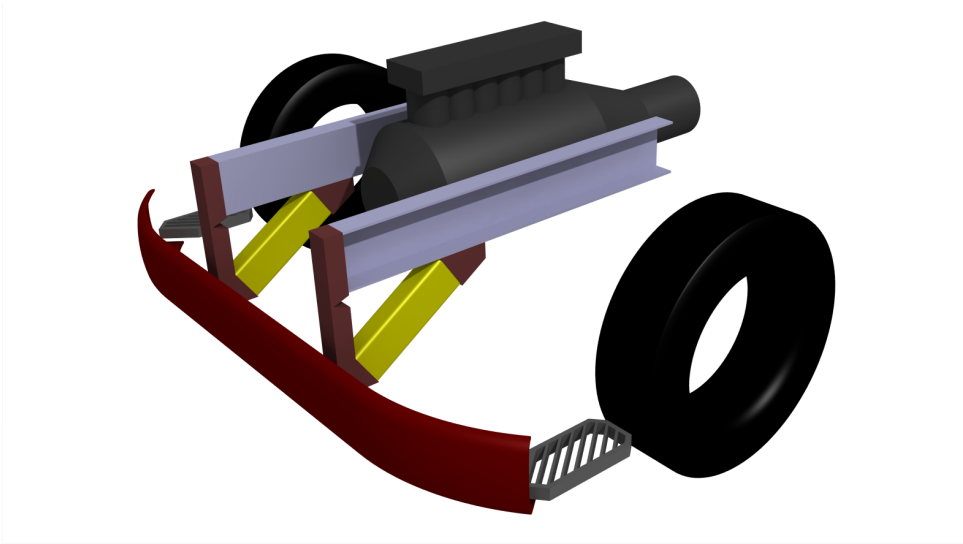

Figure 3.2: Representation of the simplified truck FE-model.

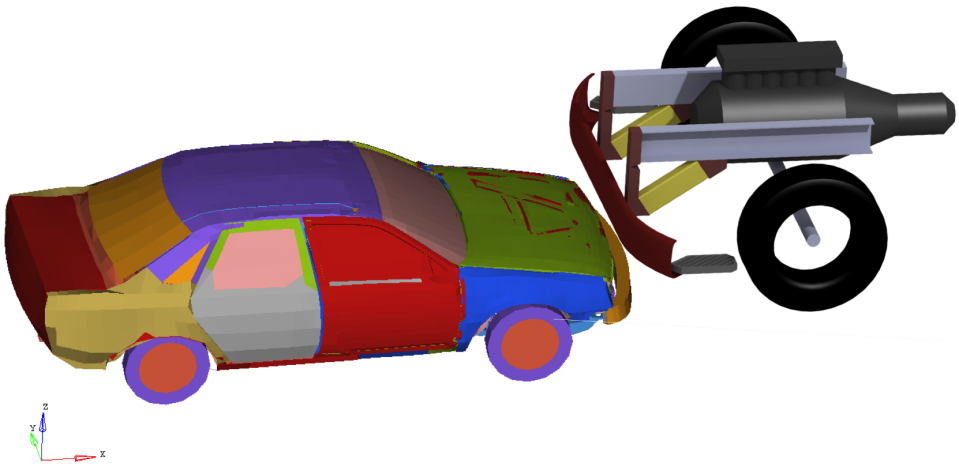

Figure 3.3: Simplified FE-model.

3.1.2 Nominal simulation

To be able to draw confident conclusions from the simplified FE-model, which was prepared in ANSA [15] and solved in LS-DYNA [16], it was important that the simplified FE-model had the same or similar response as the original Volvo Trucks FE-model, solved with RADIOSS [17]. To compare the responses of the two FE-models a nominal simulation, which is the simulation that Volvo Trucks has used to evaluate the FUPS, was used. This nominal simulation consisted of a number of fixed input parameters, *cf.* Table 3.2, used to simulate both FE-models and compare the responses to validate the behaviour of the simplified FE-model. Material input parameters were not varied in these simulations.

Table 3.2: Table of the fixed input parameters used in the nominal simulation. For definition of the parameters see Section 3.2.

$overlap$	67 %
α	0°
$v_{0,\text{truck}}$	35 km/h
$v_{0,\text{car}}$	35 km/h
m_{truck}	12000 kg
m_{car}	1400 kg
h_{off}	0 mm[iii]

The responses of the two FE-models were during the first 20 ms almost identical. It was first after 40 ms a difference could be identified. It was mainly the behaviour of the tower (for definition see Section 3.2.1) that diverted. A comparison of the two simulations showed that the tower bended less in the original FE-model, which is explained by the fact that the two cars in the two models have differences in the front structure. Thus, the behaviour of the simplified model was judged to be satisfactory.

3.2 Statistical data

The statistical data is divided into two sections, structural tolerances and collision data. Structural tolerances concern geometrical tolerances and variation of material properties in selected parts of the front of the truck, where the FUPS is mounted. The data available concerning loading conditions from accidents between trucks and cars is limited. There is rarely complete data on all the parameters chosen in this thesis from every accident and the data that exist is often catalogued in non-electronic archives. The accident data used is compiled in [18] from several different studies in Europe, see [2], [19] and [20]. The loading conditions used in the simulation are found under collision data.

3.2.1 Structural tolerances

- The variation in thickness of the FUP-beam was one of the input parameters used. The FUP-beam is the parts creating the transversal beam in the lower front section of the truck, *cf.* Figure 3.4. The thickness was estimated as the nominal thickness of the beam plus a tolerance (geometric variation) in the manufacturing process, $t_{\text{FUP-beam}} = t_{\text{nom}} + tol_{\text{FUP}}$. The variation in thickness, tol_{FUP}, was simulated with a normal distribution according to data received from the manufacturer.

[iii] Zero height offset implies that the bumper of the car meets the FUP-beam of the truck on the same height over the ground.

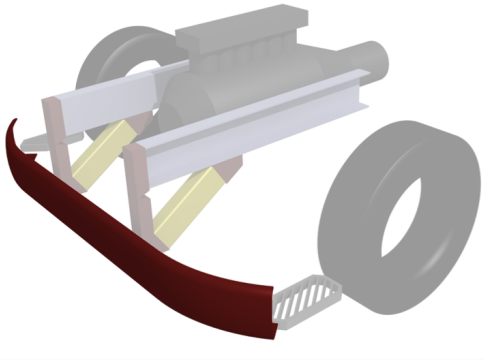

Figure 3.4: The variation in thickness of the FUP-beam was one of the parameters used in the simulation. The part highlighted shows the FUP-beam.

- The FUP-beam is attached to the truck via the tower which is hinged to the main part of the chassis, *cf.* Figure 3.5. Since the tower is made of the same material as the FUP-beam the distribution for the geometric variation in the tower is the same as for the FUP-beam.

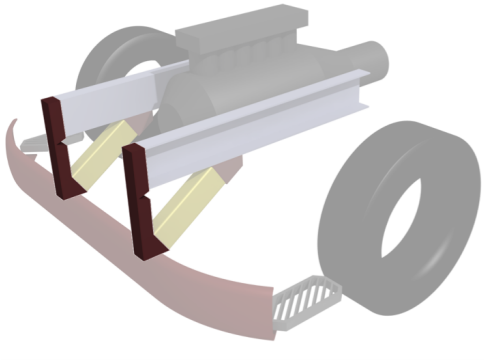

Figure 3.5: The parts highlighted are called the towers and attach the FUP-beam to the main chassis, one tower on each chassis member.

- The crash-boxes, *cf.* Figure 3.6, are the parts in the structure supposed to absorb a large part of the energy absorbed by the FUPS in a collision. The variation in thickness of the crash-boxes were distributed according to data supplied by the material manufacturer.

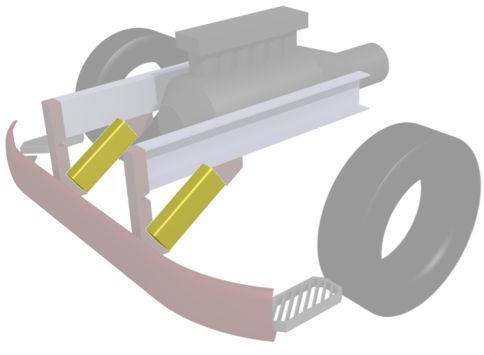

Figure 3.6: The parts highlighted shows a schematic design of the two crash-boxes, which are attached behind the FUP-beam at P2 (*cf.* Figure 4.4) and in the main chassis.

- The yield stress of the materials of the FUPS can in the manufacturing process vary. These variations were in the simulations distributed according to data supplied by the material manufacturers.

3.2.2 Collision data

- The collision angle α was considered to be the relative collision angle between the longitudinal axis of the vehicles, *cf.* Figure 3.7. The distribution of the collision angle is found in Figure 3.8a from [2].

- Overlap was defined as the ratio between the width of the bumper of the car that overlaps the front of the truck (x) over the total width of the bumper of the car (y), *cf.* Figure 3.7. For example, if the car collides with the complete width of the bumper into the front of the truck, the overlap is 100 %. The overlap was simulated according to the distribution in Figure 3.8b from [2].

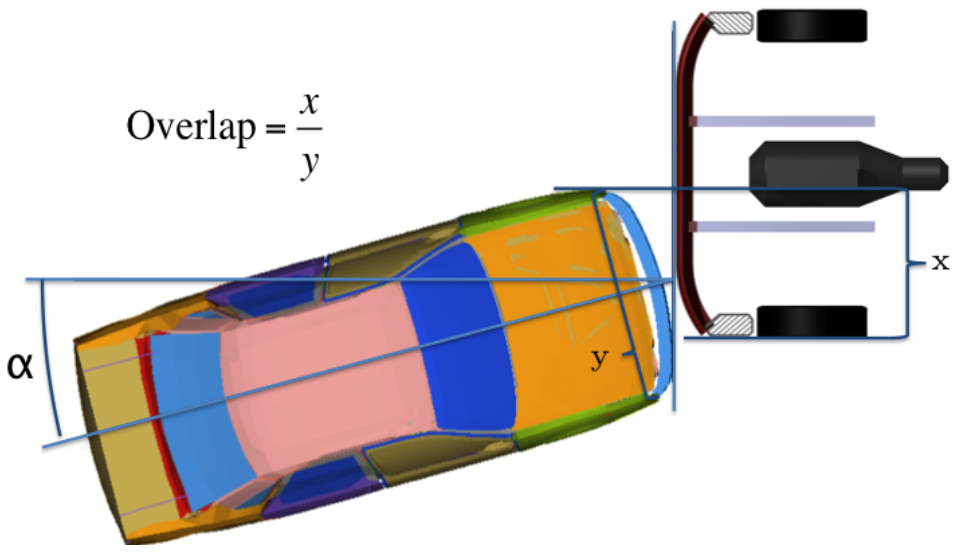

Figure 3.7: Definition of the collision angle α and the overlap.

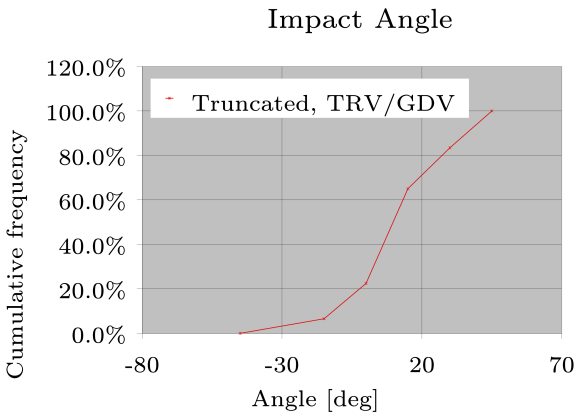

(a)

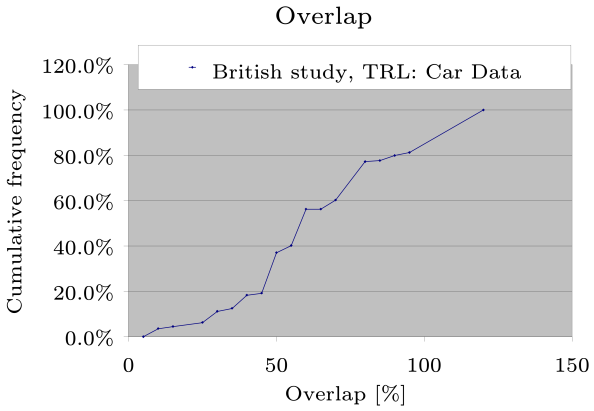

(b)

Figure 3.8: (a) shows the distribution of the collision angle. (b) shows the distribution of the vehicle overlap.

- The height offset was calculated as the difference between the height of the FUP-beam and the height of the bumper of the car. In a collision it is preferable, when considering energy absorption, if the bumper on the car and the FUP-beam on the truck are on the same height over the ground. The height from the ground to the bumper varies between different car models which results in that the bumper of the car meets the front of the truck on different heights and that can affect the response of the FUPS. The distributions for the two parameters are found in Figure 3.9 from [18].

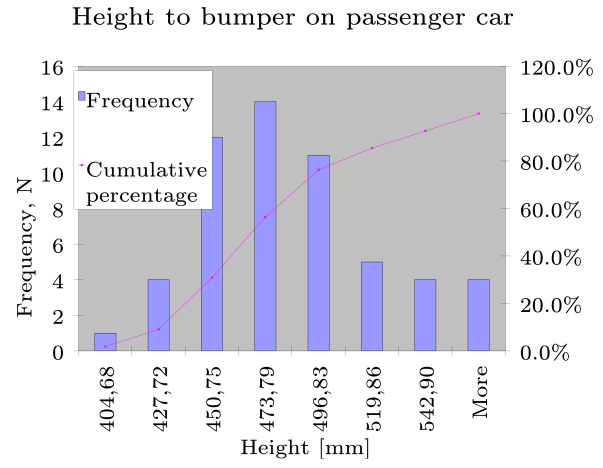

(a)

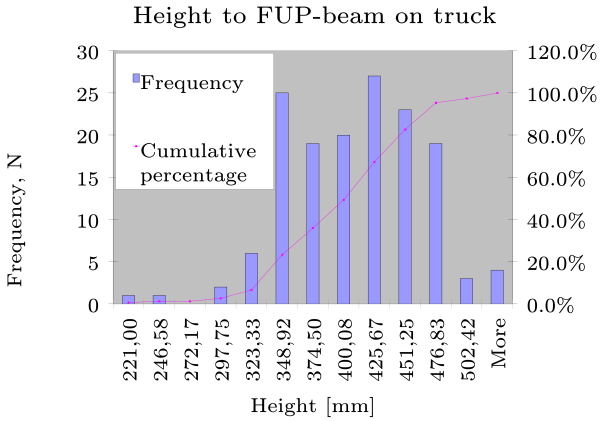

(b)

Figure 3.9: (a) and (b) show the distribution of the height over the ground for the bumper of the car and the FUP-beam, respectively.

- Since the simplified FE-model was not validated for higher energy levels than in the original Volvo Trucks model, an energy limit was needed. A limit of 250 % of the energy level in the nominal simulation was chosen since a higher energy level showed unreliable response. In the accident data received from GDV [2], outliers in the truck velocity were scratched. Example of outliers are: high velocity of the truck resulting in total demolition of both car and FUPS and low velocity of the truck resulting in no deformation and therefore no activation of the FUPS. These examples were of no interest when analysing the behaviour of this FUPS. Similarly, outliers found in the accident data of the mass of the truck and the velocity and mass of the car were scratched [2], [19] and [20]. The velocities of the truck and the car in accident data are often not specified separately, instead it is often the closing speed that is possible to calculate from an accident scene. This means that the accident velocity data available is limited. The truncated distributions used in the sampling are found in Figure 3.10 and 3.11.

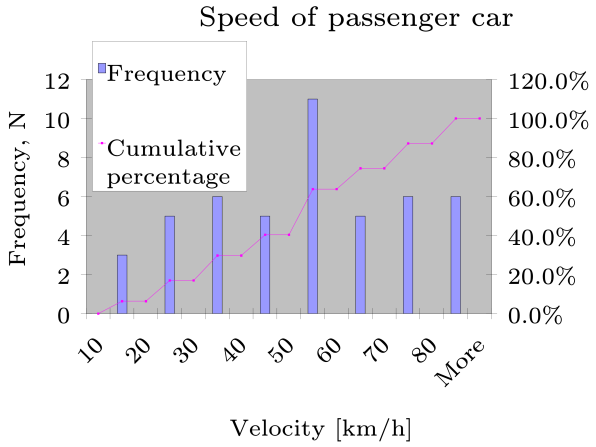

(a)

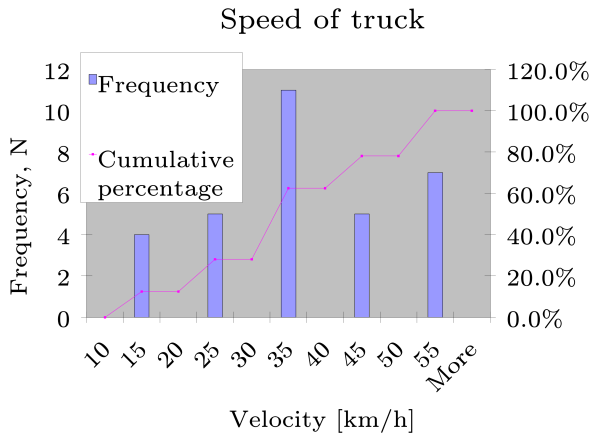

(b)

Figure 3.10: Truncated distributions of the collision velocities of the car (a) and truck (b).

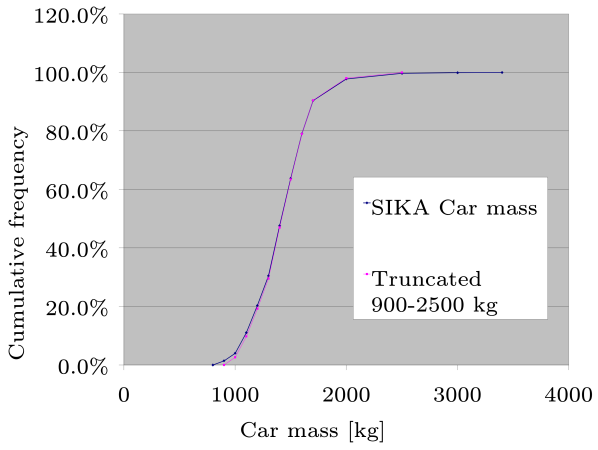

(a)

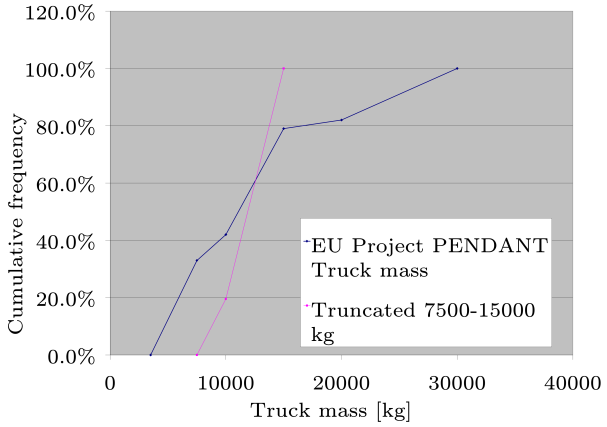

(b)

Figure 3.11: Truncated distributions of the masses of the car (a) and truck (b). (The velocities are converted to m/s before simulation.)

3.3 Simulation process

When the purpose is to run a large number of simulations with different input variables, a software is preferable to use. In LS-OPT it is possible to choose a number of different sampling techniques that generate values from specified distributions for the defined input variables.

Two types of stochastic simulations have been performed; one kept fixed at the same energy level as in the nominal simulation and one with an energy interval of 20-250 % of the level in the nominal simulation. The first one was made to be a comparison to the nominal simulation while the latter to examine the response of the FUPS in a wider energy range. According to the statistical data in Section 3.2 the nominal simulation is in the lower part of the energy spectra of real-world accidents while a robustness and reliability study of a FUPS should include at least a large part of the entire spectra. In the fixed energy analysis the velocities and masses of both truck and car were set to the nominal values and in the variable energy simulation a constraint was set on the sampled energy level to conform to the specified levels.

3.4 Analysis of response

The Monte Carlo analysis resulted in several response points in a multidimensional response space and the analysis tools in Chapter 2 can be used to view and evaluate such data. Slices through the response space produce *scatter plots* (also called *anthill plots*) which show the sample sets in 2D- or 3D-plots (for convenience only 2D-plots are printed in this thesis).

3.4.1 Stored responses

The robustness analysis of a system requires that the pertinent responses have been measured during the simulation. There is a problem to know in advance which responses that are important to store, especially when only a point value is sampled in each simulation, *e.g.*, the maximum internal energy in a structural part, and not the entire energy history. Several points of the same response can be sampled at different time steps, but since it is a problem to know the behaviour of the FUPS at a certain time step, these values can be hard to compare between simulations (with different input parameters). A valuable tool to choose responses to sample can be a specification of demands and input from test engineers, since the resulting statistical data is easy to compare to data from physical experiments [5].

In the analysis of the this FUPS the responses in Table A.1 (Appendix A) have been sampled during analysis. These responses were the same in both the fixed and the variable energy analyses, except the total energy response E, which is redundant when the energy level is fixed. The number of responses are high and not all of them have been used in the results but can be taken as examples of possible responses to sample.

3.4.2 Post-processing strategy

Two types of analyses have been performed, *i.e.*, reliability and robustness analyses. The first is a method of measuring the reliability in different response variables, *i.e.*, the probability and corresponding confidence interval of fail or success for a given event in a variable. In this thesis this has been set up as a fictive (in lack of information on real values) specification of demands in Table A.2, where the parameters investigated were chosen as the important ones for this specific FUPS, however, other parameters could be examined. The robustness analysis consists of two parts, where the first is evaluating the distribution of the individual responses, which could be called the quantitative analysis. The second is an analysis of the overall behaviour and is in this thesis performed in a straightforward manner; the scatter plots of the responses are examined manually on a high level to see tendencies in the overall response, see Figures A.3 to A.5. Interesting individual scatter plots are viewed closer and finally certain simulation runs are examined to explain their position in the scatter plots.

4 Results

This chapter covers the results produced from simulation as well as results from the literature studies of the utilisation of robust CAE. The reliability and robustness in CAE is handled first with the reliability analysis of the FUPS following this. The chapter ends with the robustness analysis.

4.1 Robustness and reliability in CAE

Robustness of a system could be, as mentioned above, a measure of the system performance from expected and unexpected events. A Dictionary of Computing [21] defines it as:

"A measure of the ability of a system to recover from error conditions, whether generated externally or internally; for example, a robust system would be tolerant to errors in input data or to failures of internal components. Although there may be a relationship between robustness and reliability, the two are distinct measures: a system never called upon to recover from error conditions may be reliable without being robust; a highly robust system that recovers and continues to operate despite numerous error conditions may still be regarded as unreliable in that it fails to provide essential services in a timely fashion on demand."

As defined here there is often a connection between robustness and reliability but also a clear distinction. The Oxford Dictionary of English [22] defines the reliability in a broad sense as:

"Consistently good in quality or performance; able to be trusted: a reliable source of information."

Clearly the definitions have a degree of overlap but in the statistical sense the reliability of a system is to the risk of failure (or rather success of proper performance) while the robustness is a measure of the ability to function even thought numerous errors occur.

For the analysis of a crash protective system like FUPS both measures are valuable, however, since no failure state has been defined for the system the resulting analysis will be a robust one. When specification of demands has been set up, these could be interpreted as the states that are accepted and the simulation responses ending up outside the demands as failure states; in this way a reliability study can be performed.

Both robustness and reliability are based on analyses that span the loading space and Monte Carlo analysis is therefor a pertinent tool for both studies.

The definitions above give no information about a quantitative measure of robustness and reliability. This is also a problem with most literature on the subject. While reliability can be examined with defined failure state and resulting confidence for system success the robustness is somewhat harder to define. In [5] the skewness and kurtosis of a system response are suggested as a measure. For example, a response showing high positive skewness is characterized by limit states, located in the right portion of the PDF, which might be either an advantage or disadvantage depending on the application. A system with high level of kurtosis is a system, which has only a few operational states with high probability while remaining do not, and it is important to see whether these probable states are desirable or not. In either case spiky character of the PDF suggests that jumps between operation states can occur.

Another view of a quantitive measure of robustness would be the lack of quantification,

i.e., if the system response shows such a strong randomness that it cannot be fitted with any regression model the system behaves in a non-robust manner.

In lack of other mathematical tools the review of engineers is invaluable for examining resulting data and making a qualitative rating of the system robustness. However, mathematical tools will be helpful to guide the engineer in this evaluation.

A type of non-robust behaviour that may need manual handling is the presence of outliers, those points outside the five finger summary. These are responses that are not typical to the rest and may be the indication of a system that has an alternative operation mode, which is especially the case if there is a cluster of outliers present. Outliers can sometimes be disregarded as improper response, and there are various rules for doing this, however, this should be done with caution since they sometimes provide important information about unusual circumstances in the system [6].

When the robustness of two systems are to be compared a problem arises; if quantification of robustness is difficult then consequently the comparison of these is even harder. Along with this a problem is that the result often is depending on the input variables and not just the system model. For example, if the input variables in an analysis have either a normal or uniform distribution the distribution of the response will most likely be different. A solution to this could be to standardise the simulation and thus excluding this source of variation, then the qualitative and quantitative robustness of two or more systems can be compared.

4.1.1 Robust CAE methodology

In Section 3.4.2 the strategy used in this thesis was given but more elaborate schemes can be adopted. Examples can be found in [5], [8], [23] and [24] and some commercial software has been developed to perform robust analyses, *e.g.*, LS-OPT [25] and optiSLang [26]. In Figure 4.1 a scheme combined from several sources is shown.

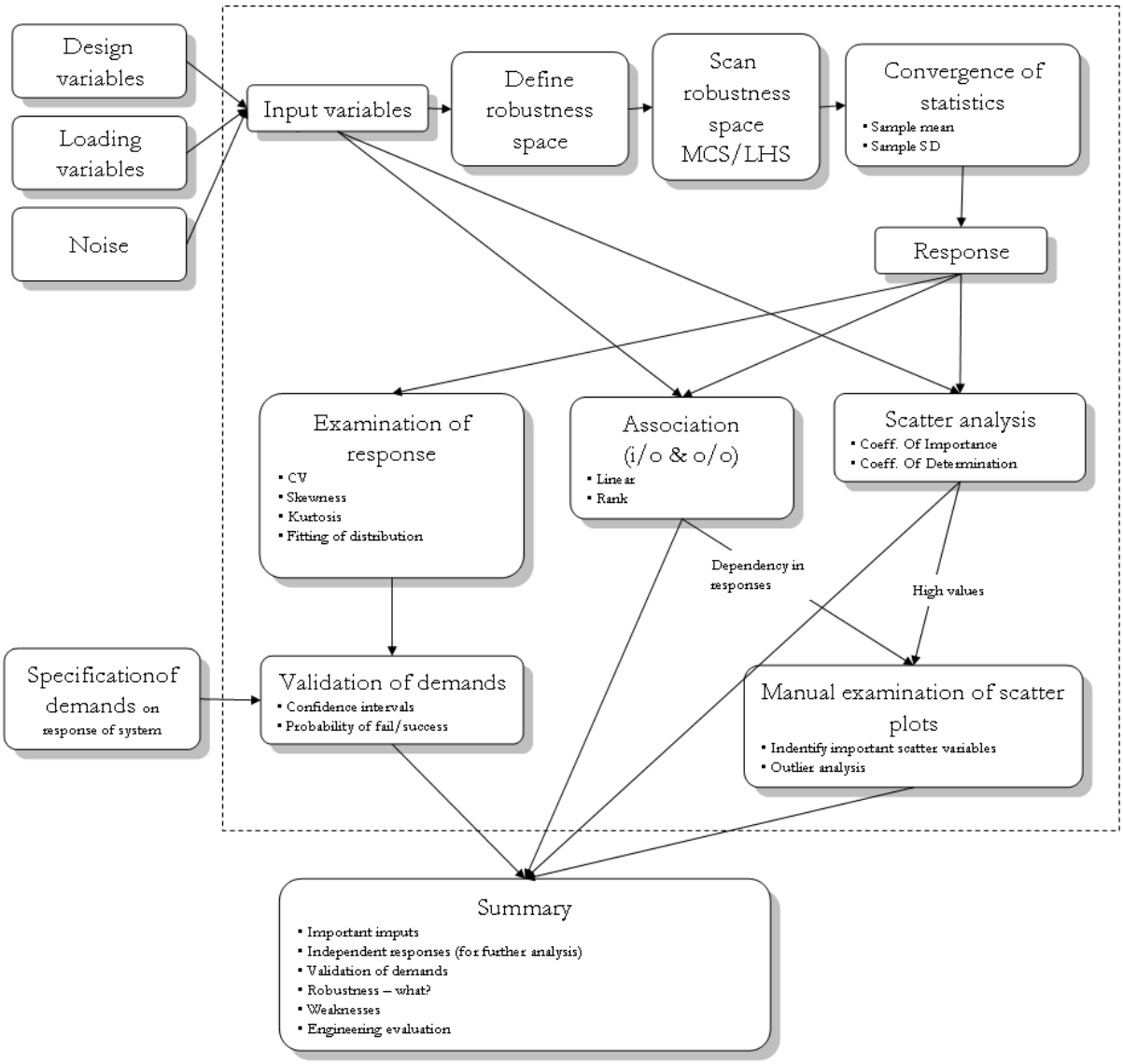

Figure 4.1: Possible strategy to adopt when performing robust CAE.

4.2 Reliability analysis

The reliability analysis is performed on the parameters specified in Table A.2 and in this section the probabilities to meet the demands are examined. The probabilities presented below is calculated from the simulation with the energy interval of 20-250 % of the nominal simulation.

- $F_{\mathrm{LH,CB}}$ and $F_{\mathrm{RH,CB}}$: The section force limit in the crash-boxes during a collision was set to 180 kN. It was set as a desire and computed as 120 % of the trigger force 150 kN, a level chosen by Volvo Trucks based on UN ECE-R93 § 3.3.4. [3]. Higher force indicates local peaks and incorrect buckling. The probability of success can be found in Equations 4.1 and 4.2 and in Figures 4.2a and 4.2b, respectively.

$$P[F_{\mathrm{LH,CB}} < 180 \text{ kN}] = 0.34 \tag{4.1}$$

$$P[F_{\mathrm{RH,CB}} < 180 \text{ kN}] = 0.97 \tag{4.2}$$

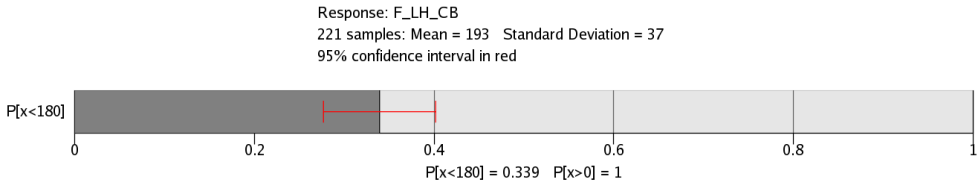

(a)

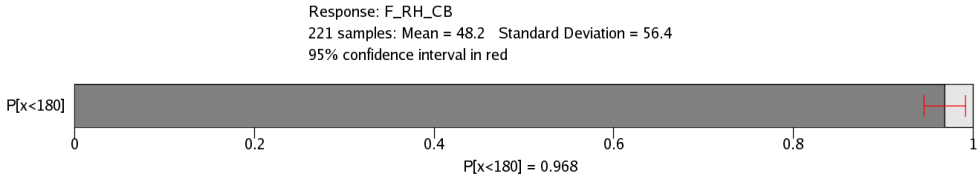

(b)

Figure 4.2: Probability of maximum section force in left (a) and right (b) crash-boxes.

- $F_{\mathrm{P1,X}}$, $F_{\mathrm{P2,X}}$ and $F_{\mathrm{P3,X}}$: The points P1, P2 and P3 are situated in the front of the FUP-beam and indicate different load application points used when certification testing is performed. These are placed between the end and the middle of the beam, as seen in Figure 4.4, and the longitudinal contact force subjected by the car in each point can be compared with the force levels in UN ECE-R93 § 3.3.4. [3]. Hence these probabilities are not used as a reliability measurement but rather a indication of how well the forces in an accident compare to the certification forces. The probability of success can be found in Equations 4.3 to 4.5 and in Figure 4.3.

$$P[F_{\mathrm{P1,X}} < 80 \text{ kN}] = 0.50 \tag{4.3}$$

$$P[F_{\mathrm{P2,X}} < 160 \text{ kN}] = 0.75 \tag{4.4}$$

$$P[F_{\mathrm{P3,X}} < 80 \text{ kN}] = 0.72 \tag{4.5}$$

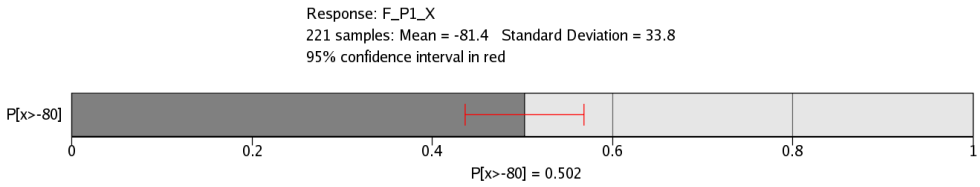

(a)

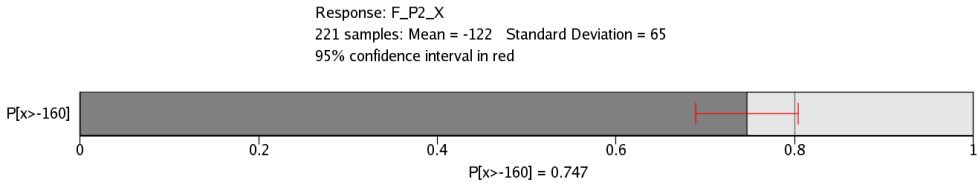

(b)

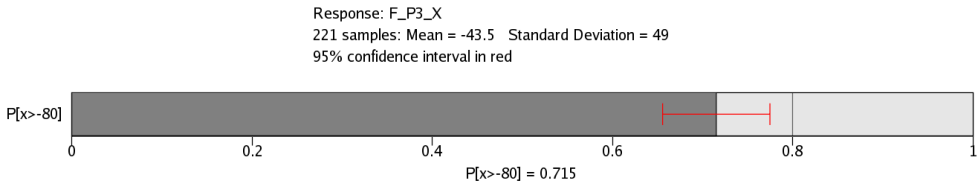

(c)

Figure 4.3: Probability of having contact forces in P1, P2 and P3 lower than the corresponding certification force levels. Note that the negative sign is due to the definition of the contact and can be directly translated to the probabilities in Equations 4.3 to 4.5.

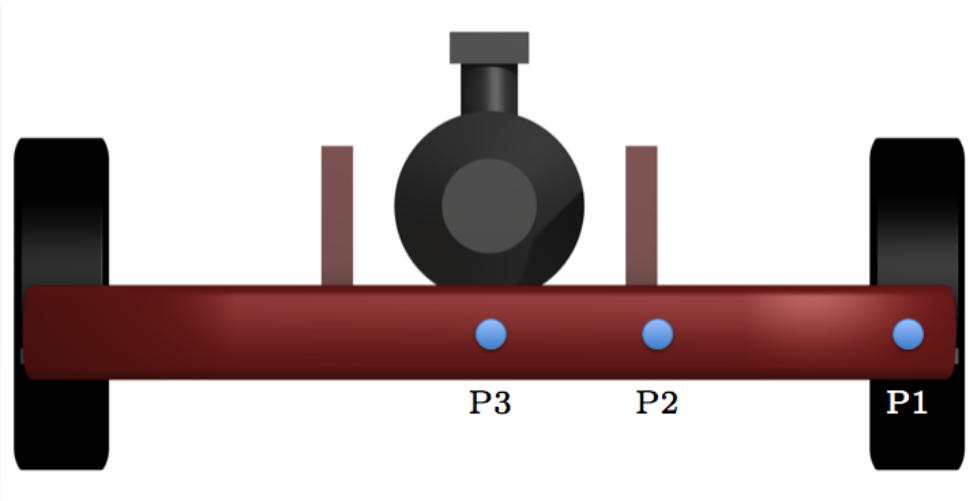

Figure 4.4: The testing points P1, P3 and P3 on the left hand side of the FUP-beam.

- $F_{\mathrm{tire,FUP}}$: A contact between the FUPS (with instep) and the tire of the truck is unwanted and a nonzero contact force between these is an indication that the FUPS has hit the tire. Because of noise the force level was set at 1 kN rather than 0 when calculating the probability that the FUPS has not touched the tire in Equation 4.6 and Figure 4.5.

$$P[F_{\mathrm{tire,FUP}} < 1 \text{ kN}] = 0.20 \tag{4.6}$$

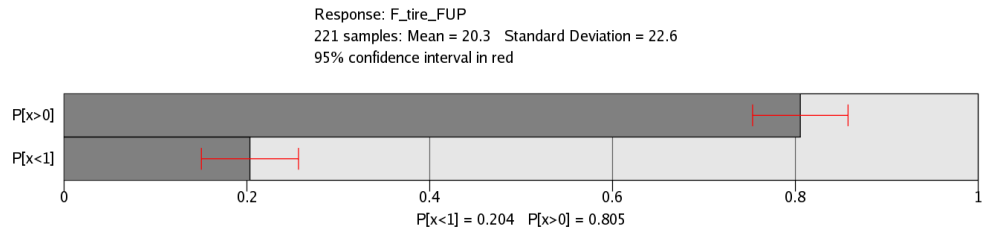

Figure 4.5: Probability of having low, almost no, contact force between the FUPS (with instep) and the tire.

- $F_{\text{tire,car}}$: Compared to the contact between the FUPS and the tire an even more dangerous scenario is if the truck looses the possibility to steer. This is likely if the car hits the tire of the truck. Therefore a demand of no contact (also 1 kN as above) was set for the force between the car and the tire. The probability function is found in Equation 4.7 and the probability plot is found in Figure 4.6.

$$P[F_{\text{tire,car}} < 1 \text{ kN}] = 0.50 \tag{4.7}$$

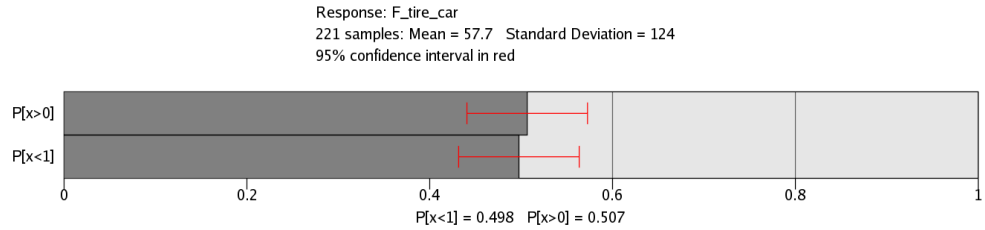

Figure 4.6: Probability of the car not hitting the tire of the truck.

- $r_{\text{E,int,truck}}$: The desired level for the ratio between the internal energy of the truck and the total internal energy in a collision was set to be in the interval of 20 % and 80 %. The lower boundary is set low but still better than no energy absorbed as it is in today's solutions. The probability is found in Equation 4.8 and the probability plot is found in Figure 4.7.

$$P[0.2 < r_{\text{E,int,truck}} < 0.8] = 0.69 \tag{4.8}$$

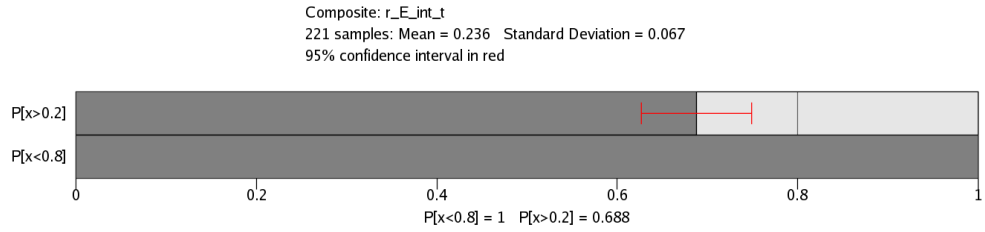

Figure 4.7: Probability of maximum fraction of absorbed energy in truck over the total absorbed energy in the collision.

- $r_{\text{E,CB}}$: The crash-boxes function is to absorb energy in a head-on collision. The crash-boxes are designed to buckle in a specific manner and thereby absorb as much energy

as possible. The ratio between the internal energy in the crash-boxes and the internal energy in the truck was set to be between 30 % and 100 %. The upper level of the desire, to be able to absorb 100 % of the trucks internal energy in the crash-boxes, would mean that the only part damaged in a collision would be the crash-boxes which of course is more of a utopia. The probability is found in Equation 4.9 and plotted in Figure 4.8.

$$P[0.3 < r_{\mathrm{E,CB}} < 1.0] = 0.23 \tag{4.9}$$

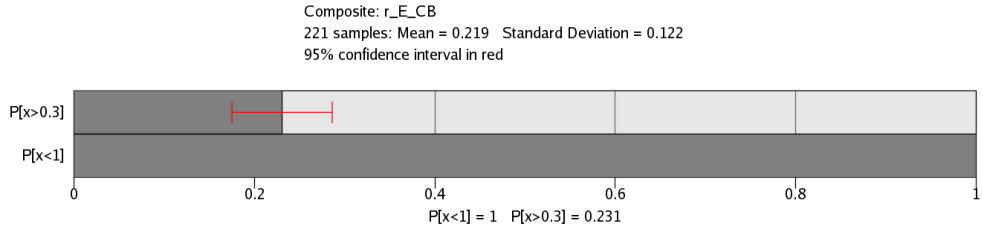

Figure 4.8: Probability of maximum fraction of absorbed energy in the crash-boxes over the total absorbed energy in the truck.

- $r_{\mathrm{E,FUP-beam}}$: The ratio between the internal energy in the FUP-beam and the internal energy in the truck was set to a desired level of 0 % to 30 %, because high energy would be a sign of large deformations which is unwanted in the FUP-beam. The probability of achieving this is found in Equation 4.10, *cf.* Figure 4.9 for probability plot.

$$P[r_{\mathrm{E,FUP-beam}} < 0.3] = 0.63 \tag{4.10}$$

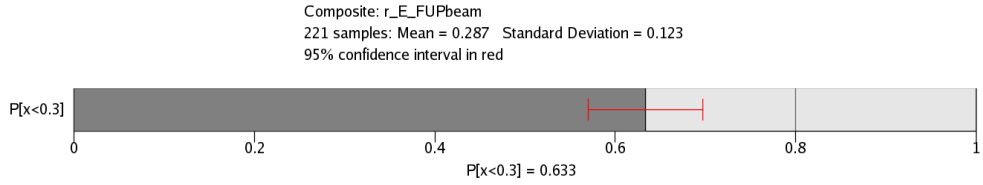

Figure 4.9: Probability of maximum fraction of absorbed energy in the FUP-beam over the total absorbed energy in the truck.

- $r_{\mathrm{E,tower}}$: The ratio between the internal energy in the towers and the internal energy in the truck was set to be in the interval 0 % to 20 %, because high energy would be a sign of large deformations which is unwanted also in the tower, see Equation 4.11, *cf.* Figure 4.10

$$P[r_{\mathrm{E,tower}} < 0.2] = 0.98 \tag{4.11}$$

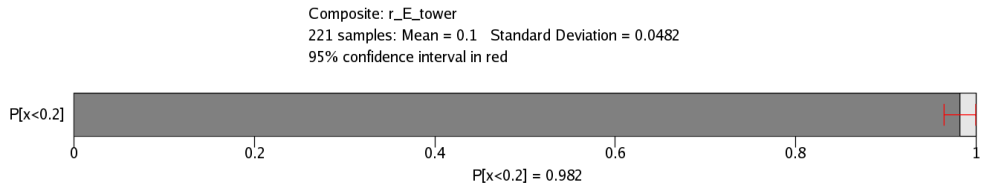

Figure 4.10: Probability of maximum fraction of absorbed energy in the towers over the total absorbed energy in the truck.

- $\delta L_{\text{beam,LH}}$, $\delta L_{\text{beam,RH}}$: The longitudinal deformation of the two longitudinal beams in the front part of the car was given a limit of 500 mm. The original length of the beams was 960 mm. This is the deformation zone of the car and therefore where the most energy should be absorbed by the car. The probability plots are found in Figure 4.11 and the probability in Equation 4.12 and 4.13.

$$P[\delta L_{\text{beam,LH}} < 500 \text{ mm}] = 0.43 \tag{4.12}$$

$$P[\delta L_{\text{beam,RH}} < 500 \text{ mm}] = 0.74 \tag{4.13}$$

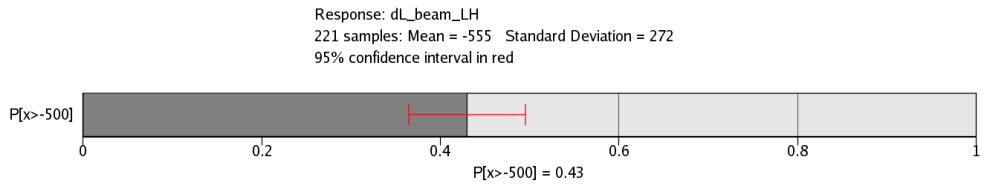

(a)

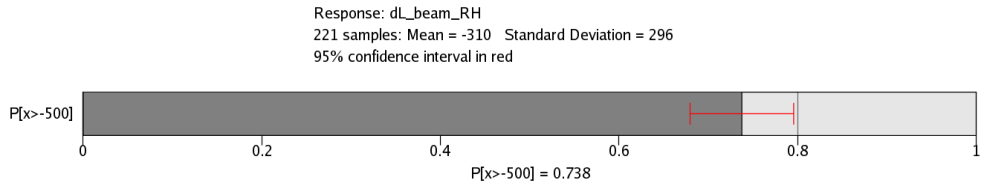

(b)

Figure 4.11: Probability of less than maximum compression of the front longitudinal beams in the car.

- $intr_{\text{P1}}$, $intr_{\text{P2}}$, $intr_{\text{P3}}$: The intrusions at P1, P2 and P3 (*cf.* Figure 4.4) are regulated by UN ECE-R93 §8.3 [3], where a maximum distance of 400 mm between the frontmost part of the truck and a given point is allowed after certification testing has been performed (*cf.* Figure A.1). Based on this and the geometry of the front of the truck, the allowed intrusion levels were calculated to 287, 367 and 376 mm for P1, P2 and P3 respectively. The probabilities and the probability plot for these are found in Equation 4.14 to 4.16 and Figure 4.12.

$$P[intr_{\text{P1}} < 287 \text{ mm}] = 0.45 \tag{4.14}$$

$$P[intr_{\text{P2}} < 367 \text{ mm}] = 0.98 \tag{4.15}$$

$$P[intr_{\text{P3}} < 376 \text{ mm}] = 1 \tag{4.16}$$

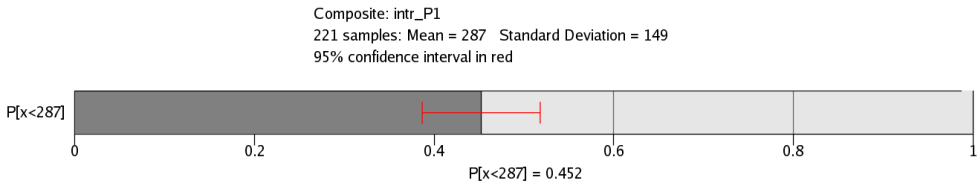

(a)

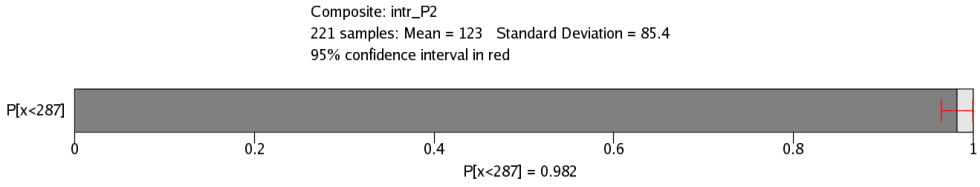

(b)

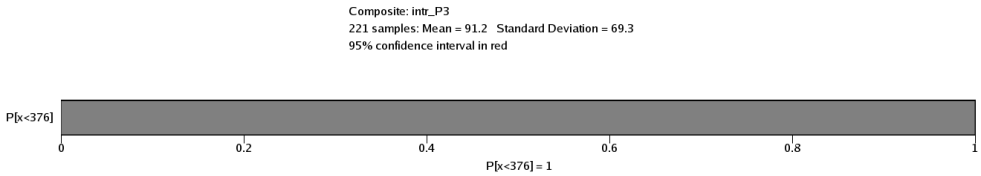

(c)

Figure 4.12: Probability of less than maximum intrusion at P1, P2 and P3.

- δy_{P1}: The lateral displacement of P1 is regulated by UN ECE-R93 §10.9 [3], where the outermost part of the FUP-beam may not displace outside the mudguards or end up more than 100 mm inside the outmost part of the wheel (*cf.* Figure A.2). Since the outermost part of the FUP-beam was not logged this was translated to an interval of -50 mm to 35 mm lateral displacement for P1. The probability of success is found in Equation 4.17 and displayed in Figure 4.13.

$$P[-50 \text{ mm} < \delta y_{\mathrm{P1}} < 35 \text{ mm}] = 0.25 \tag{4.17}$$

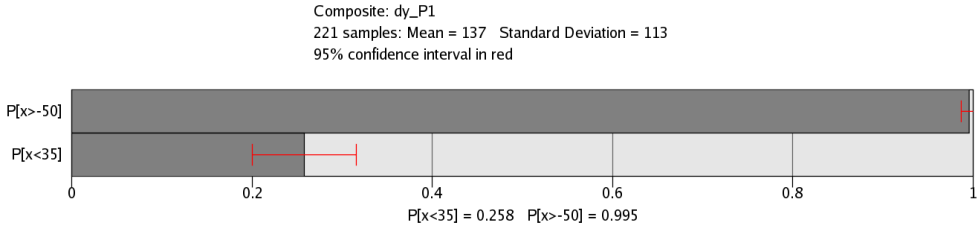

Figure 4.13: Probability of maximum lateral displacement at P1.

- δy_{P2}: This parameter was used to indicate erroneous crash-box buckling which is when the displacement in the point is high. The probability is found in Equation 4.18 and the probability plot is found in Figure 4.14.

$$P[-10 \text{ mm} < \delta y_{\mathrm{P2}} < 60 \text{ mm}] = 0.85 \tag{4.18}$$

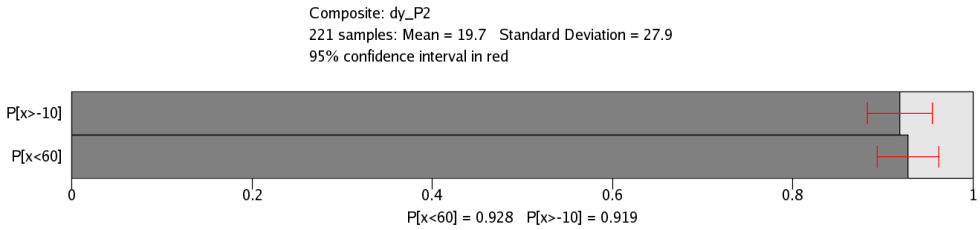

Figure 4.14: Probability of maximum lateral displacement at P2.

- δz_{P1} , δz_{P2}, δz_{P3}: The vertical displacement in P1, P2 and P3 is regulated by UN ECE-R93 §8.7 [3], where the ground clearance may never exceed 450 mm (*cf.* Figure A.1), which gives a maximum displacement of 120 mm upwards for this FUPS. Probability plots are found in Figure 4.15 and the probability is found in Equation 4.19 to 4.21.

$$P[\delta z_{\mathrm{P1}} < 120 \text{ mm}] = 0.88 \tag{4.19}$$

$$P[\delta z_{\mathrm{P2}} < 120 \text{ mm}] = 1 \tag{4.20}$$

$$P[\delta z_{\mathrm{P3}} < 120 \text{ mm}] = 1 \tag{4.21}$$

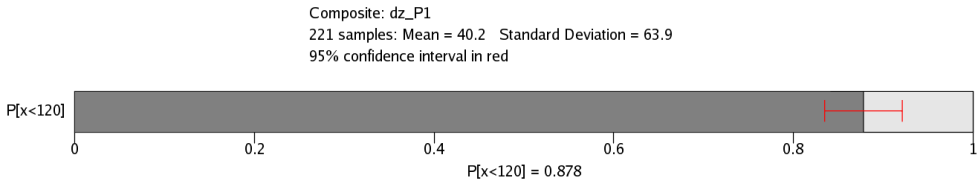

(a)

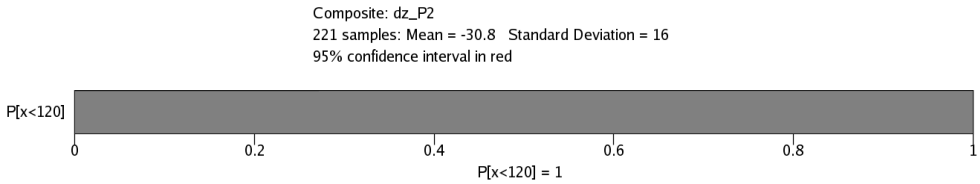

(b)

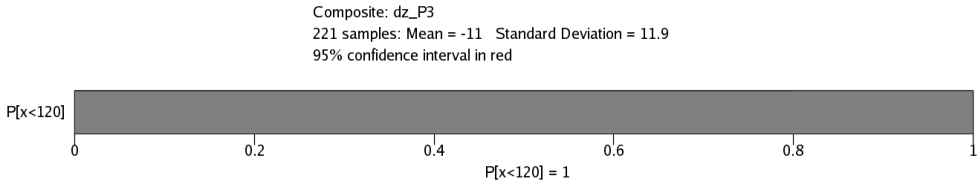

(c)

Figure 4.15: Probability of the vertical displacement in P1, P2 and P3 respectively.

4.3 Robustness analysis

In this section the analysis of the FUPS robustness is covered, *i.e.*, quantitative and qualitative analyses are made of the responses from the Monte Carlo simulation. The responses examined below are defined in Table A.1.

4.3.1 Energy absorption

When developing an EA-FUPS the level of kinetic energy transformed into heat by friction (referred to as energy absorption) is of course important and a pertinent start for the robustness evaluation. While a high and robust level of total absorbed energy in the truck is desirable in all EA-FUPS the level of the individual parts of the system is also important. Particularly in the present system, which has crash-boxes designed to absorb most of the energy. The following results are taken from the fixed energy simulation and later on in this section data from the free energy simulation will be presented.

The internal energy fractions' PDF:s, plotted as histograms in Figures 4.16 to 4.18, shows both a spiky behaviour and limiting states. When the total absorbed energy of the truck is concerned, a spiky behaviour with distinct operational states is not desirable (*cf.* Section 4.1). These states can be derived from the level of absorbed energy in the crash-boxes as seen in Figure 4.17 and are connected to the compression of these. The histogram of the intrusion of P2 in Figure 4.18, shows a first, highly probable, operational state at around 70 mm, where the crash-box is not activated and a second, less probable, state at around 200 mm with full compression. Even when the crash-boxes are activated it is not certain that the absorbed energy is high (*cf.* Figure 4.19), which can be explained by an improper buckling of the crash-box due to, *e.g.*, weak attachments between the crash-boxes and the main chassis.

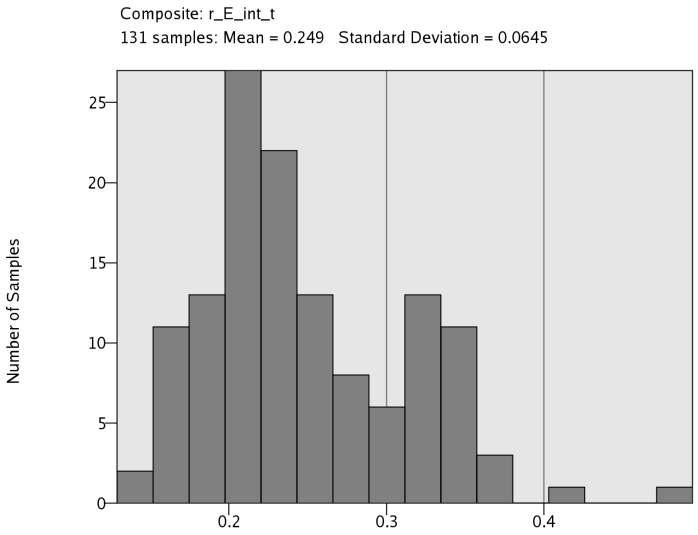

Figure 4.16: Histogram of absorbed energy of the truck $r_{\mathrm{E,int,truck}}$, showing a spiky form with two highly probable states around 0.22 and 0.34. The values above 0.4 are results of simulations where low amounts of energy has been absorbed over all and not because of high level of absorbed energy in the truck. The distribution has a skewness of 0.74 and a kurtosis of 0.44.

The scatter plot of the amount of total internal energy absorbed by the truck shows a non-increasing tendency with the overlap in Figure 4.20. When the overlap is low only one crash-box is activated and as the overlap increases the other will be as well. However, when comparing the energy absorbed in the crash-boxes to the overlap in Figure 4.21 this does not increase linearly. In fact the amount of spread is much larger for high overlaps and this is because the activation of the crash-boxes becomes more uncertain as stated in the paragraph above (*cf.* Figure 4.18).

This is confirmed by studying the intrusion at left P2 against overlap in Figure 4.22 where the compression of the left crash-box increases with overlap up to about 60 % after

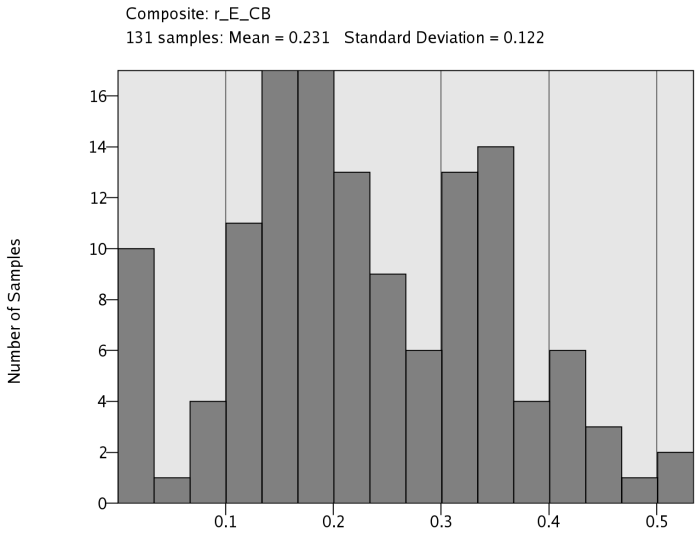

Figure 4.17: Histogram of absorbed energy in the truck $r_{\mathrm{E,CB}}$, showing a spiky form with two highly probable states around 0.17 and 0.34. The distribution has a skewness of 0.13 and a kurtosis of -0.46.

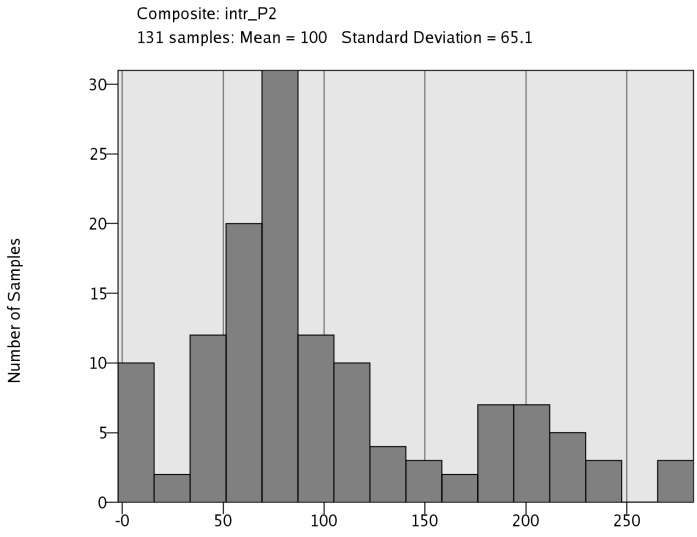

Figure 4.18: Histogram of intrusion at P2 in the truck $intr_{\mathrm{P2}}$, showing a spiky form with two highly probable states around 70 mm and 200 mm. The distribution has a skewness of 0.90 and a kurtosis of 0.07.

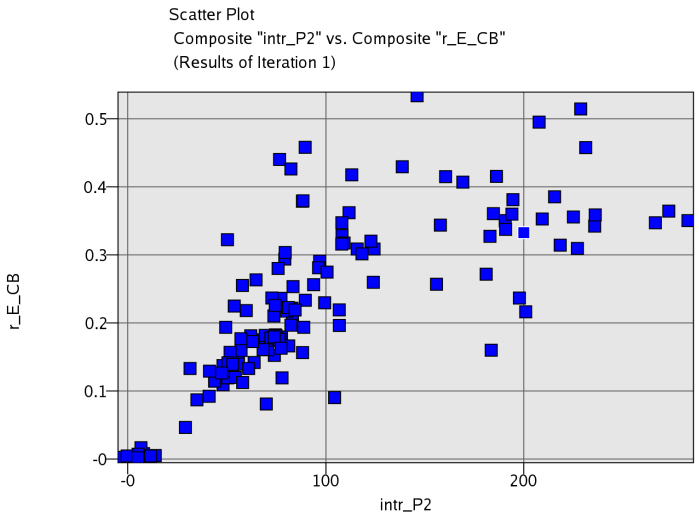

Figure 4.19: Scatter plot of absorbed energy in the crash-boxes $r_{\mathrm{E,CB}}$ and intrusion of P2 $intr_{\mathrm{P2}}$ showing a wider spread of the level of absorption as the intrusion increases.

which it shows lower levels. In Figure 4.23 there is a strong negative correlation between the compression of the left crash-box and the height offset showing that a high impact point does not activate the crash-boxes (*cf.* Figure 4.18).

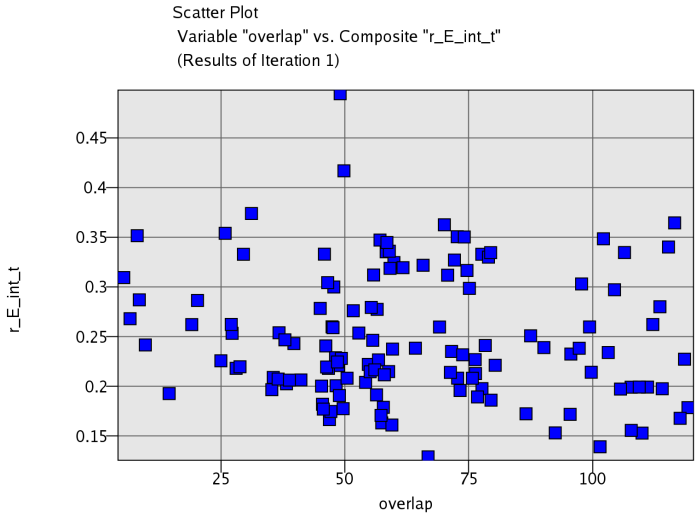

Figure 4.20: Scatter plot of absorbed energy in the truck $r_{\mathrm{E,int,truck}}$ and overlap. (*N.B.*: values of $r_{\mathrm{E,int,truck}}$ above 0.4 for the same reason as in Figure 4.16.)

4.3.2 Geometric function

Another behaviour seen in Figure 4.21 is that below 25 % of overlap no energy is absorbed in the crash-boxes, while Figure 4.20 and 4.24 shows that energy is absorbed somewhere in the FUPS. This is explained in Figure 4.25, where the FUP-beam clearly absorbs energy for overlaps beneath 25 %. This indicates that large deformations occur in the FUP-beam, which is supposed to be stiff and transport the displacement out at the end to the crash-boxes. This is clearly not the case when the FUP-beam bends instead. This behaviour can also be seen in Figure 4.26 where it is clear that there are much larger deformations in P1 than P2 and that P2 does not follow the intrusion at P1. The negative correlation between

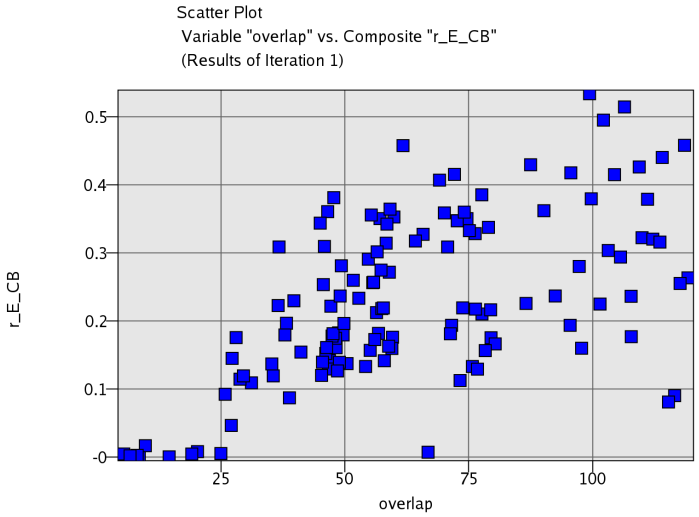

Figure 4.21: Scatter plot of absorbed energy in the crash-boxes $r_{\mathrm{E,CB}}$ and overlap.

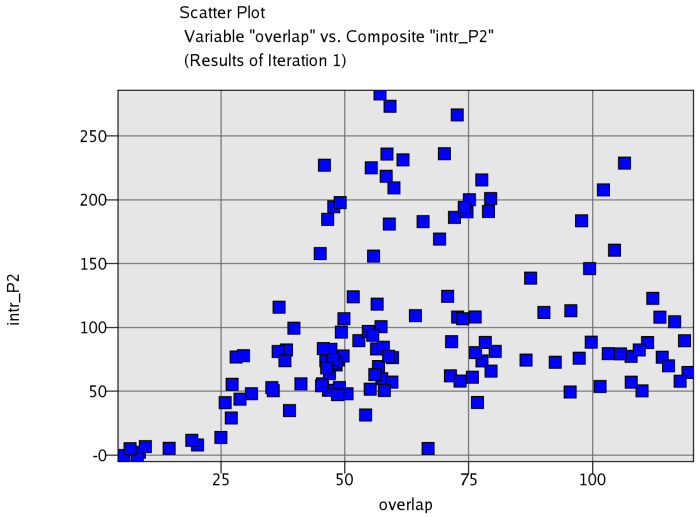

Figure 4.22: Scatter plot of the intrusion at P2 $intr_{\mathrm{P2}}$ and overlap.

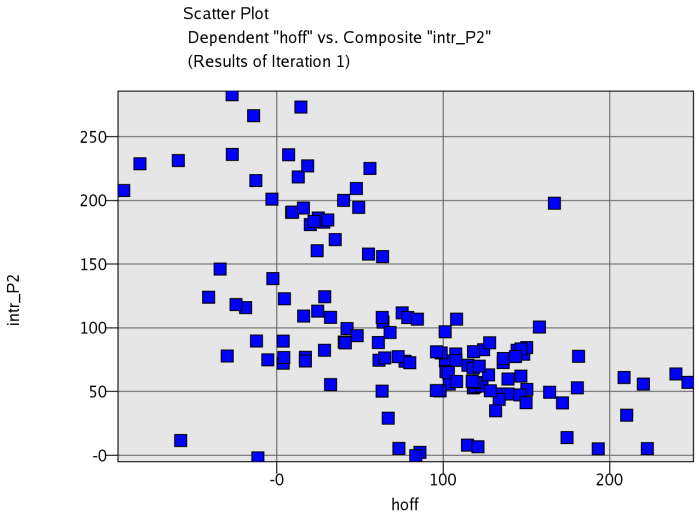

Figure 4.23: Scatter plot of the intrusion at P2 $intr_{\mathrm{P2}}$ and height offset between car bumper and FUP-beam h_{off}.

energy absorption in the crash-boxes and the FUP-beam, seen in Figure 4.27, tells that bending of the FUP-beam results in a lower level of absorbed energy in the crash-boxes.

In Figure 4.28 and 4.29 the forces on the tire is plotted showing forces capable of destroying the suspension.

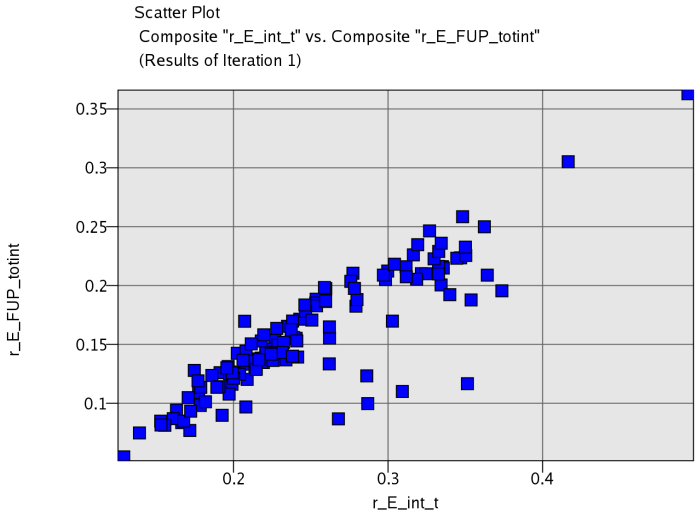

Figure 4.24: Scatter plot of total absorbed energy in the FUPS $r_{\mathrm{E,FUP,totint}}$ (*N.B.*: fraction of total internal energy in the collision) and absorbed energy in the truck $r_{\mathrm{E,int,truck}}$.

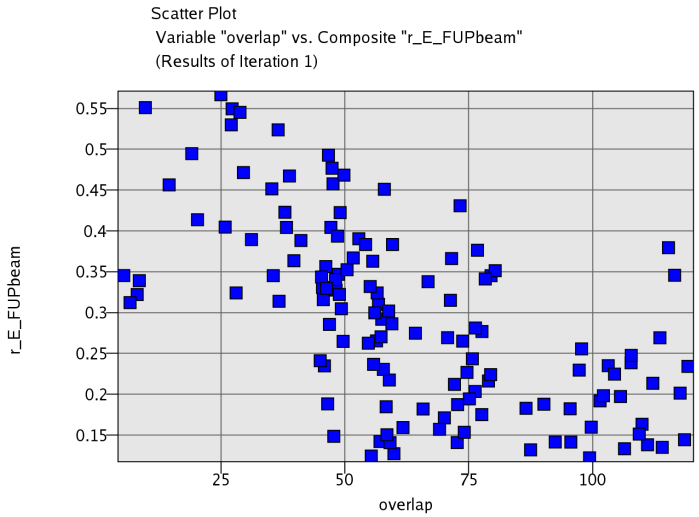

Figure 4.25: Scatter plot of absorbed energy in the FUP-beam $r_{\mathrm{E,FUP-beam}}$ and overlap.

4.3.3 Input dependencies

Figures A.6 to A.8 shows the linear correlations between the input variables and the response in the simulations with free energy levels. These are used to find dominating input parameters into the system.

- Structural tolerances: There are low correlations (almost none over 0.1) between the structural input parameters and the response. Some parameters shows slightly higher correlations, but are still rather low. For example the yield strength of the FUP-beam σ_{y} shows a slight correlation to the displacements in P1 and P3 and the force level in the left crash-box $F_{\mathrm{LH,CB}}$, which has been covered in the section above.

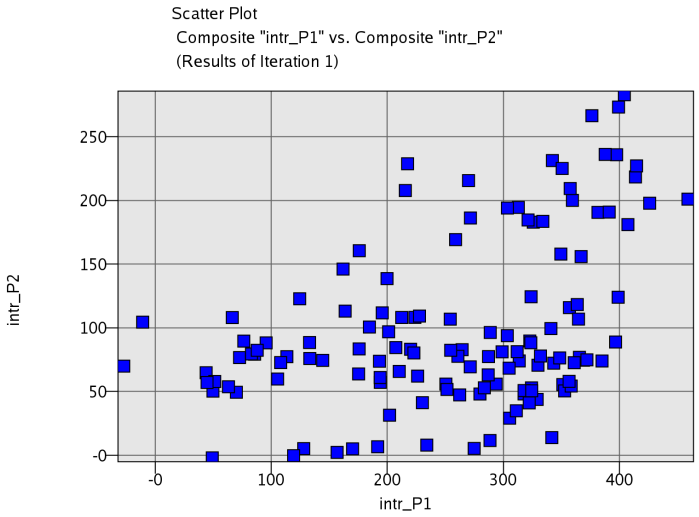

Figure 4.26: Scatter plot of the intrusion at P2 and P1. Note that the maximum value of the intrusion in P1 is twice as high as in P2.

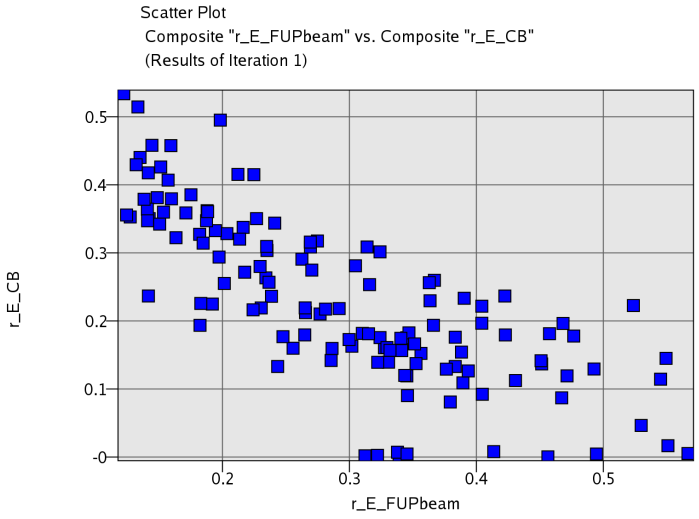

Figure 4.27: Scatter plot of absorbed energy in the crash-boxes $r_{\mathrm{E,CB}}$ and the FUP-beam $r_{\mathrm{E,FUP-beam}}$.

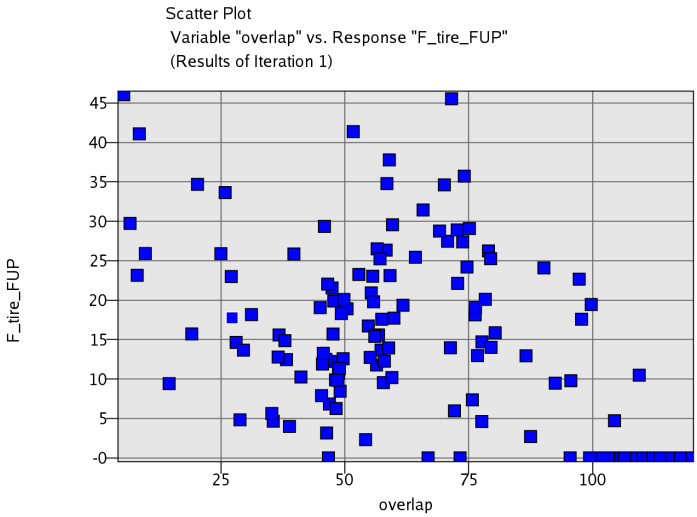

Figure 4.28: Scatter plot of forces on the left tire subjected by the FUPS (and instep) $F_{\text{tire,FUPS}}$ against overlap.

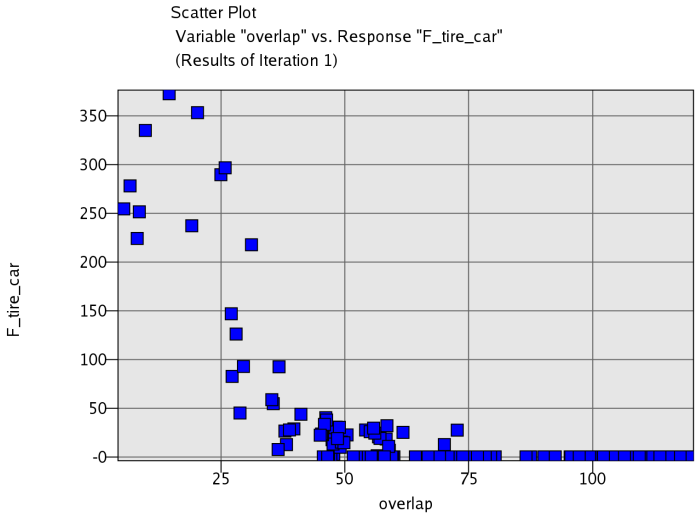

Figure 4.29: Scatter plot of forces on the left tire subjected by the car $F_{\text{tire,car}}$ against overlap.

- Collision data: Most of the influence of collision data has been covered in the section above, however, some correlations can be observed. Since the level of the initial kinetic energy is directly connected to severeness of the collision the mass and energy have strong correlations to several responses that can represent this. Because of the large difference in mass between the vehicles the initial velocity of the truck $v_{0,\mathrm{t}}$ has much larger impact on the crash results than the initial velocity of the car $v_{0,\mathrm{c}}$.

5 Conclusions

This chapter presents the conclusions made from the results. The conclusions concern Robust CAE, Reliability and Robustness of the analysed FUPS.

5.1 Robust CAE

The usage of robust CAE is a pertinent tool for many engineering problems, especially when the input domain contains large amount of uncertainties. When used early in the development of a new system it can be used to explore the design space and give knowledge about the most robust and reliable designs. There are also many tools, *e.g.*, PCA, available to improve a systems robustness and examinations of the statistics on the response informs the engineer more about the design than mere deterministic analysis would.

When it comes to grading of the system performance the reliability is easy to quantify while the robustness is hard to give an appropriate value. As seen in the figures of distributions (*cf.* Figures 4.16 to 4.18) the skewness and kurtosis give some assistance in finding non-robust behaviour in this application. If the system goes through an improvement process where the system is altered in a way that changes the robustness and then simulated with the same input it is possible to quantitatively compare the response, but if two systems are analysed differently it is hard to do this. To create a useful grading system for a system like FUP it requires some sort of standardised analysis, where the measure is set. This standard analysis could consist of the input from accidents used in this thesis but the responses and measure of these would need to be evolved.

In any case the robustness analysis should be performed in a software dedicated to this task, so that the engineer can be properly guided and letting the handling of the numerous response points be made easier.

5.2 Reliability of the analysed FUPS

It is important to remember that the probabilities presented are estimations based on a limited number of accidents because of the infrequent documentation of all the input parameters used in the simulations.

- Since input data for the simulation was based on accident data on roads with right-hand traffic, the probability of successfully reaching the trigger force in the crash-boxes is higher for the left crash-box compared to the right. The section force in the right crash-box in an accident will most probably be below the set limit while the probability to be below the limit in the left crash-box was estimated to 34 %. This means that 66 % of all accidents show high force levels which could indicate spiky behaviour and incorrect buckling or no buckling at all of the left hand crash-box.

- The longitudinal contact forces in P1, P2 and P3 (*cf.* Figure 4.4) are likely to be below the certification levels in UN ECE-R93 § 3.3.4. [3], which indicates that these forces should be used with caution when designing trigger forces for an EA-FUPS. As seen in Equation 4.4 there is a 75 % risk of having a trigger force below 160 kN in P2.

- There is an 80 % risk of the instep to hit the wheel of the truck, which is a well known problem. This is why the attachment of the instep should be weak enough not to harm the steering but strong enough not to fatigue from everyday use. A larger problem is that there is a 50 % risk of having the car hitting the tire of truck (*N.B.*: this is a direct contact between the car and the tire and not with the FUPS

in between). It can thus be concluded that the analysed FUPS is not very good at preventing the car from hitting the tire and possibly destroying the steering.

- A car is often incapable of absorbing a high energy level in a collision with a truck without causing serious injuries to the occupants of the car. It is therefore desirable to absorb a large part of the energy in the truck in a collision. In the performed simulation the probability of having the truck absorbing 20-80 % of the energy in a collision was estimated to 69 %, which is quite high. However, the lower level should be increased to such level that the truck is capable to absorb the energy it contributes to the collision (approximately 80 % in average) in future designs.

- There is only a 23 % chance of having the crash-boxes collecting more than 30 % of the total absorbed energy in the truck, which should be considered a low reliability in the structure. Of course, the absorbed energies in the truck can be so high that the measured ratio might go down, but a part of the system that is designed with the sole purpose of absorbing energy should show high levels of doing so.

- The 63 % probability of absorbing less than 30 % of the energy in the FUP-beam indicates that the deformations in the beam are quite moderate. Unfortunately it is not known if the remaining 37 % are excessive bending of the outer end of the beam or just larger transverse compression.

- In 57 % of the simulated collisions the car's left longitudinal beam is fully compressed which means that the FUPS activates the car's own crash protective system.

- The maximum allowed intrusions in the front of the FUPS are mostly met except in P1 (the outermost point) where there is only a 45 % chance of preventing to large intrusions. This is a result of a weak FUP-beam, which bends for small overlap collisions and the fact that this point is already 90 mm further back than P2 and P3 in the undeformed FUPS. A small overlap protection systems (SOPS) could help prevent this.

- The probability of being below the maximum vertical displacements in P1, P2 and P3 are high. It is not surprising that the standard deviation is highest for P1 since the position of P1 is on the far end of the FUP-beam. The mean of the vertical displacement of P2 shows that most of the time this point actually moves downwards. This and the above conclusion mean that in most of the collisions the FUPS fulfills its prime objective, which is preventing the car from going to far under the truck even though the energy-absorbing mechanism is not activated.

5.3 Robustness of the analysed FUPS

The robustness of the Volvo FUPS has been evaluated in a straightforward manner.

- The absorbed energy shows both a spiky behaviour and a left skewness, *i.e.*, the high levels are disconnected to the lower levels and less probable. This is coupled to the activation of the crash-boxes which is far from certain. The problem has two reasons:

  - The crash-boxes in the real FUPS are not parallel with the longitudinal axis, *i.e.*, they are pointing outwards at a small angle to the left and right respectively. When colliding straight on, this angle locks the backwards motion of the FUP-beam resulting in no compression of the crash-boxes. This is also a result of a weak FUP-beam, which when hit in the middle at approximately P3 (see Figure 4.4) bends rather than transmitting the backwards motion to the crash-boxes.

  - The fact that many car bumpers have a positive height offset to the FUP-beam result in a hit in the towers and above, rather than in the beam. (*cf.* Section 3.2.)

- When the crash-boxes are activated it is not certain that the absorbed energy is high, which can be explained by an improper buckling of the crash-box due to, *e.g.*, weak attachments between the crash-boxes and the main chassis.

- A weak FUP-beam makes the FUPS loose its prime objective, to prevent cars from being overrunned by the truck, and thus the car or parts of the FUP-beam (often the instep) subject the tire of the truck to high forces. The result of this can be catastrophic for both the car, the truck and other traffic.

- A problem is the lack of high correlations between the input and the response. Besides the obvious correlations as the initial velocity of the truck $v_{0,\mathrm{t}}$ and energy in the collision, the structural variables showed low correlations. This is due to the fact that the loading variables control the collision results. Therefore, design parameters going in to a robustness analysis must be able to match the variability of the loading parameters, if they are to give any affect.

- The nominal simulation used to evaluate the original FE-model is not representative for the operating conditions for the FUPS. The choice of parameters for the nominal simulation were probably chosen to create a worst case scenario. This means that the current system is optimised for a crash scenario that is unlikely to occur.

- A major concern is that even though large resources are put into the development of EA-FUPS a rather obvious way to consume energy would be to effectively decrease the velocity of the truck before the moment of impact. Without a much larger energy absorbing mechanism on the truck that can absorb the trucks total kinetic energy in the collision (several times the car) the head-on collision between cars and trucks will be catastrophic for the car. A proper EA-FUPS combined with other systems that brake the truck can be an effective solution for saving many lives.

6 Recommendations

The most important recommendations from this thesis are:

- Involve robust CAE in the development of crash protection system; then both the system robustness and reliability can be improved. This is preferably made on an early stage when the design parameters are free to vary and really affect the robustness, as opposed this thesis, where the structural parameters are only noise.
- Build a proper input space such that the true operating conditions for the system are defined.
- Increase the stiffness of the FUP-beam.
- Try to prevent the crash-boxes to buckle improperly. This could be made by guiding the crash-box and improving the attachment at the top.
- Lower the trigger force for the crash-boxes so that theses are triggered more often. This way there is a larger chance of absorbing energy in the truck.
- For future designs the hinges connecting the tower to the main chassis should be placed higher or another system design should be implemented.
- To help preventing excessive intrusion of P1 a small overlap protection system could be installed.

References

[1] Strandroth, J., Rizzi, M. *Djupstudieanalys av olyckor med tunga lastbilar - Effekter av åtgärder för en säker tung trafik*. Vägverket, Borlänge, Sweden, 2008.

[2] Gwehenberger, J., *et al. Collection of Existing In-depth Accident Cases and Prediction of Benefit on Having Front and Rear Underrun*. GDV, Insurance Institute for Traffic Engineering, 2004.

[3] UN ECE Regulation No 93 (UN ECE R93). *Concerning the adoption of uniform conditions of approval and reciprocal recognition of approval for motor vehicle equipment and parts*. United Nations, Geneva, Switzerland, 1994.

[4] European Union. Europa Summaries of EU legislation, Accessed: 2010-10-17. Available from: `http://europa.eu/legislation_summaries/internal_market/single_market_for_goods/motor_vehicles/technical_implications_road_safety/l21248_en.htm`.

[5] Marczyk, J. *Principles of Simulation-Based Computer-Aided Engineering*. FIM Publications, Barcelona, Spain, 1999.

[6] Montgomery, D. Runger, G. *Applied statistics and probability for engineers*. John Wiley & Sons, Inc, United States of America, 2007.

[7] Bucher, C. Basic concepts for robustness evaluation using stochastic analysis. In *Efficient Methods for Robust Design and Optimization*, London, England, 2007.

[8] Roos, D. Advanced methods of stochastic and optimization in industrial applications. In *Numisheet 2008*, Interlaken, Switzerland, 2008.

[9] Zuyev, S. Personal interview, 12 April 2010.

[10] Hessenberger, K., *et al.* Robustness Investigation of a Numerical Simulation of the ECE-R14 with particular regard to correlation analysis. Stuttgart, Germany, 2005.

[11] Stander, N., *et al. LS-Opt User's Manual*. Livermore software technology corporation, Livermore, California, USA, 2010.

[12] Smith, L. A tutorial on principal components analysis, 2002.

[13] Cook, R., *et al. Concepts and applications of finite element analysis*. John Wiley & Sons, 1989.

[14] Bathe, K-J. *Finite element procedures*. Prentice Hall, 1996.

[15] Beta CAE Systems S.A. ANSA, Accessed: 2010-07-19. Available from: `http://www.beta-cae.gr/ansa.htm`.

[16] LSTC. LS-Dyna, Accessed: 2010-07-19. Available from: `http://www.lstc.com/lsdyna.htm`.

[17] Altair. RADIOSS, Accessed: 2010-08-05. Available from: `http://www.hyperworks.in/(S(ftp4gr3sbminmpypwhrrbrzz))/HWTemp1Product.aspx?product_id=51&AspxAutoDetectCookieSupport=1`.

[18] Krusper, A. & Thomson, R. Crash Compability Between Heavy Goods Vehicles and Passenger Cars: Structural Interaction Analysis and In-Depth Accident Analysis. Paris, France, May 19-22 2008. Proceedings of International Conference on Heavy Vehicles.

[19] SIKA. FORDON 2008_090611.xls, Accessed: 2010-11-03. Available from: `http://www.sika-institute.se/Doclib/2009/Statistik/FORDON%202008_090611.xls`.

[20] Lenard, J. *et al.* PENDANT: a European crash injury database. Paper presented at the 2nd Expert Symposium on Accident Research. Hannover, Germany, September 1-2 2006.

[21] Daintith, J. and Wright, E., editors. *A Dictionary of Computing.* Oxford University Press, 2008. Available from: `http://www.oxfordreference.com/views/ENTRY.html?subview=Main&entry=t11.e4532` [cited 2010-07-26].

[22] Soanes, C. and Stevenson, A., editors. *The Oxford Dictionary of English (revised edition).* Oxford University Press, 2008. Available from: `http://www.oxfordreference.com/views/ENTRY.html?subview=Main&entry=t140.e65064` [cited 2010-07-26].

[23] Will, J. & Stelzmann, U. Robustness Evaluation of Crashworthiness using LS-DYNA and optiSLang. Congress Center Dresden, Germany, November 21-23 2007. ANSYS Conference & 25$^{\text{th}}$ CADFEM Users' Meeting.

[24] Nunes, R. F. *et al.* Robustness Evaluation of brake systems concerned to squel noise problem. Weimarer Optimerungs- und Stochastiktage 6.0, October 15-16 2009.

[25] LSTC. LS-Opt, Accessed: 2010-07-19. Available from: `http://www.lstc.com/lsopt.htm`.

[26] Dynardo. optiSLang, Accessed: 2010-08-04. Available from: `http://www.dynardo.de/en/software/optislang/`.

A Figures and tables

The figures and tables that could not be fitted within the report can be found below.

Table A.1: Table of stored responses in each simulation run.

Parameter		**Sampling**	**Filter, unit**
$F_{\text{LH,CB}}$	Section force left crash-box	Resultant, Max	SAE300, ms
$F_{\text{RH,CB}}$	Section force right crash-box	Resultant, Max	SAE300, ms
$F_{\text{P1,X}}$	Longitudinal contact force in P1	X-dir, Min	SAE300, ms
$F_{\text{P2,X}}$	Longitudinal contact force in P2	X-dir, Min	SAE300, ms
$F_{\text{P3,X}}$	Longitudinal contact force in P3	X-dir, Min	SAE300, ms
$F_{\text{tire,FUP}}$	Contact force between left tire and FUP	Resultant, Max	SAE300, ms
$F_{\text{tire,car}}$	Contact force between left tire and car	Resultant, Max	SAE300, ms
E	Total energy in simulation.	At $t = 0.00ms$	none
r_{E}	$\frac{E}{632228 \text{ (original energy level)}}$	At $t = 0.00ms$	none
$r_{\text{E,int}}$	$\frac{\text{total internal energy}}{\text{total energy}}$	Max	none
$r_{\text{E,kin}}$	$\frac{\text{total kinetic energy}}{\text{total energy}}$	Min	none
$r_{\text{E,int,truck}}$	$\frac{\text{internal energy of truck}}{\text{total internal energy}}$	Max	none
$r_{\text{E,int,car}}$	$\frac{\text{internal energy of car}}{\text{total internal energy}}$	Max	none
$r_{\text{E,CB}}$	$\frac{\text{internal energy of crash-box}}{\text{total internal energy of truck}}$	Max	none
$r_{\text{E,FUP}-\text{beam}}$	$\frac{\text{internal energy of FUP-beam}}{\text{total internal energy of truck}}$	Max	none
$r_{\text{E,tower}}$	$\frac{\text{internal energy of tower}}{\text{total internal energy of truck}}$	Max	none
$r_{\text{E,FUP,totint}}$	$\frac{E_{\text{tower}}+E_{\text{FUP}-\text{beam}}+E_{\text{CB}}}{\text{total internal energy}}$	Max	none
$\delta L_{\text{beam,LH}}$	Compression of left longit. car beam	Min	none
$\delta L_{\text{beam,RH}}$	Compression of right longit. car beam	Min	none
$intr_{\text{P1}}$	Intrusion at left P1	Last value	none
$intr_{\text{P2}}$	Intrusion at left P2	Last value	none
$intr_{\text{P3}}$	Intrusion at P3	Last value	none
δy_{P1}	Lateral displacement of left P1	Last value	none
δy_{P2}	Lateral displacement of left P2	Last value	none
δy_{P3}	Lateral displacement of P3	Last value	none
δz_{P1}	Vertical displacement of LH P1	Last value	none
δz_{P2}	Vertical displacement of LH P2	Last value	none
δz_{P3}	Vertical displacement of P3	Last value	none
$v_{\text{x,car}}$	final x-velocity of car in local coord.	Last value	none
$v_{\text{y,car}}$	final y-velocity of car in local coord.	Last value	none
$v_{\text{X,truck}}$	final x-velocity of car in global coord.	Last value	none
$v_{\text{Y,truck}}$	final y-velocity of car in global coord.	Last value	none

Table A.2: Example of specification of demands used in the reliability analysis of responses.

Parameter	Lower limit	Upper limit	Demand/Desire	P[success]
Forces				
$F_{\mathrm{LH,CB}}$		180 kN	Desire	0.34
$F_{\mathrm{RH,CB}}$		180 kN	Desire	0.97
$F_{\mathrm{P1,X}}$		80 kN		0.50
$F_{\mathrm{P2,X}}$		160 kN		0.75
$F_{\mathrm{P3,X}}$		80 kN		0.72
$F_{\mathrm{tire,FUP}}$		1 kN	Demand	0.20
$F_{\mathrm{tire,car}}$		1 kN	Demand	0.50
Energies				
$r_{\mathrm{E,int,truck}}$	0.2	0.8	Desire	0.69
$r_{\mathrm{E,CB}}$	0.3	1	Desire	0.23
$r_{\mathrm{E,FUP-beam}}$	0	0.3	Desire	0.63
$r_{\mathrm{E,tower}}$	0	0.2	Desire	0.98
Intrusions				
$\delta L_{\mathrm{beam,LH}}$		500 mm	Demand	0.43
$\delta L_{\mathrm{beam,RH}}$		500 mm	Demand	0.74
$intr_{\mathrm{P1}}$		287 mm	Demand	0.45
$intr_{\mathrm{P2}}$		367 mm	Demand	0.98
$intr_{\mathrm{P3}}$		376 mm	Demand	1
Displacements				
δy_{P1}	-50 mm	35 mm	Demand	0.25
δy_{P2}	-10 mm	60 mm	Demand	0.85
δz_{P1}		120 mm	Demand	0.88
δz_{P2}		120 mm	Demand	1
δz_{P3}		120 mm	Demand	1

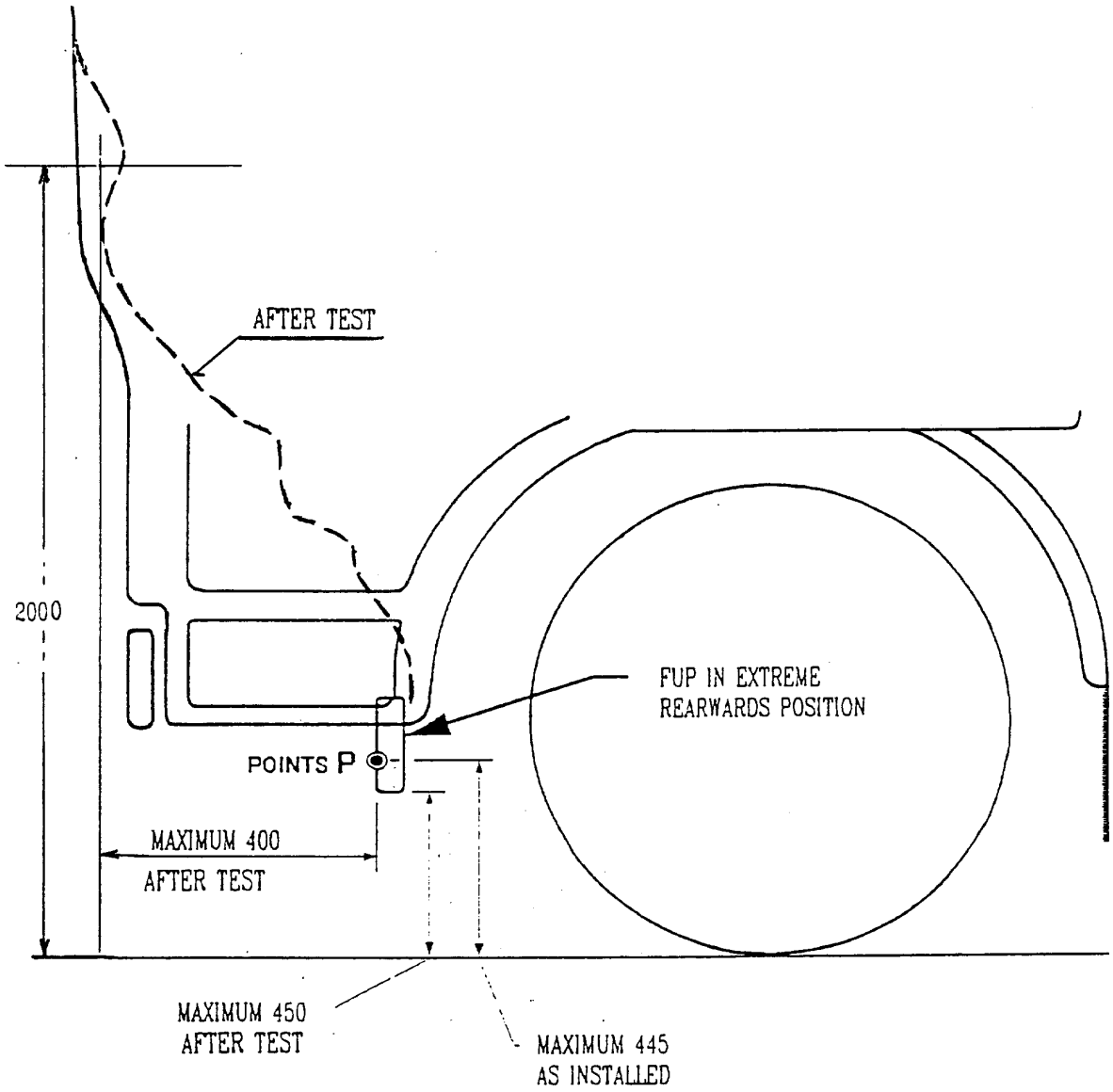

Figure A.1: Left side view of schematic FUPS including measurements. (from UN ECE-R93 Part III [3])

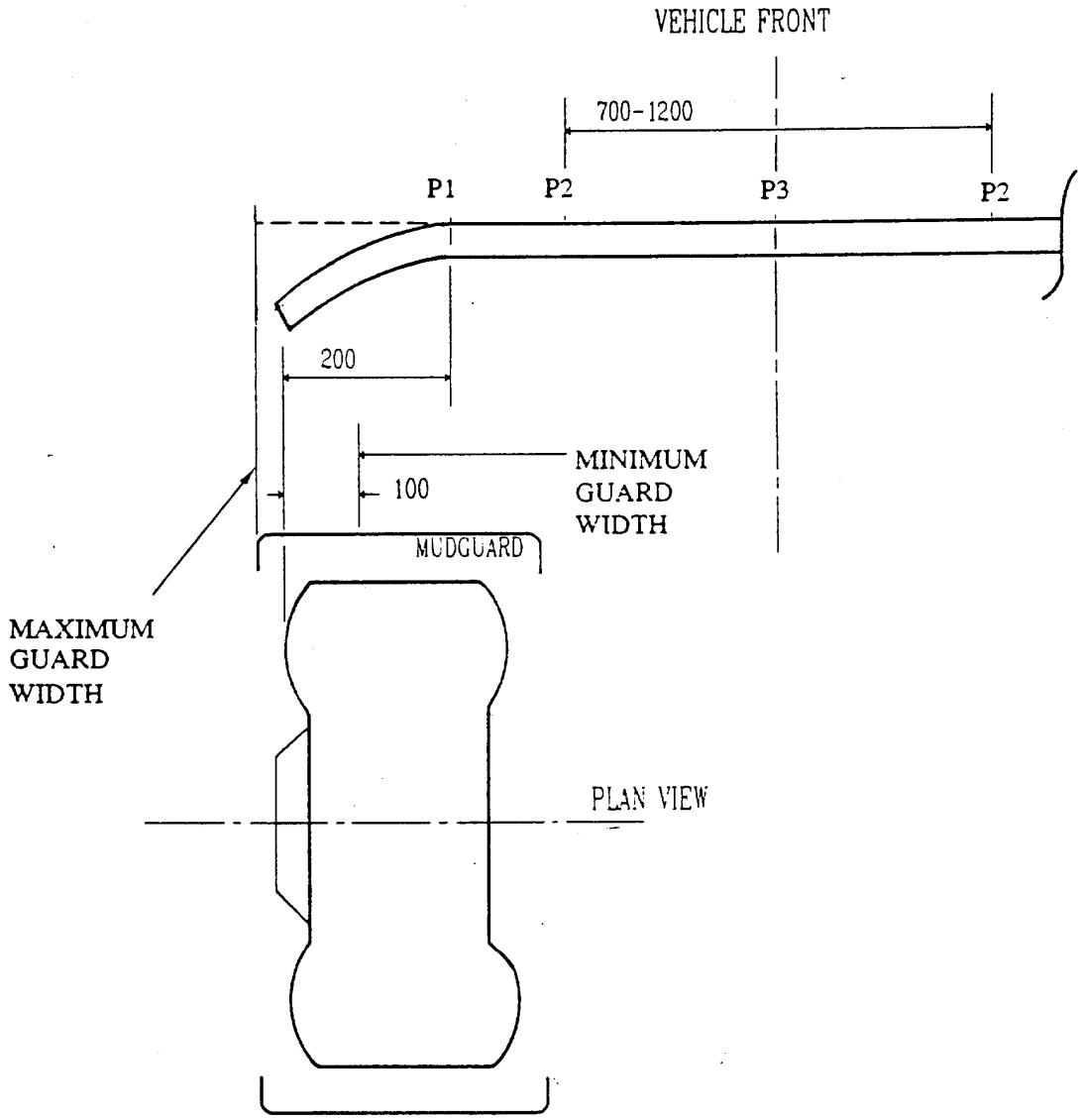

Figure A.2: Top view of schematic FUPS including measurements. (from UN ECE-R93 Part III [3])

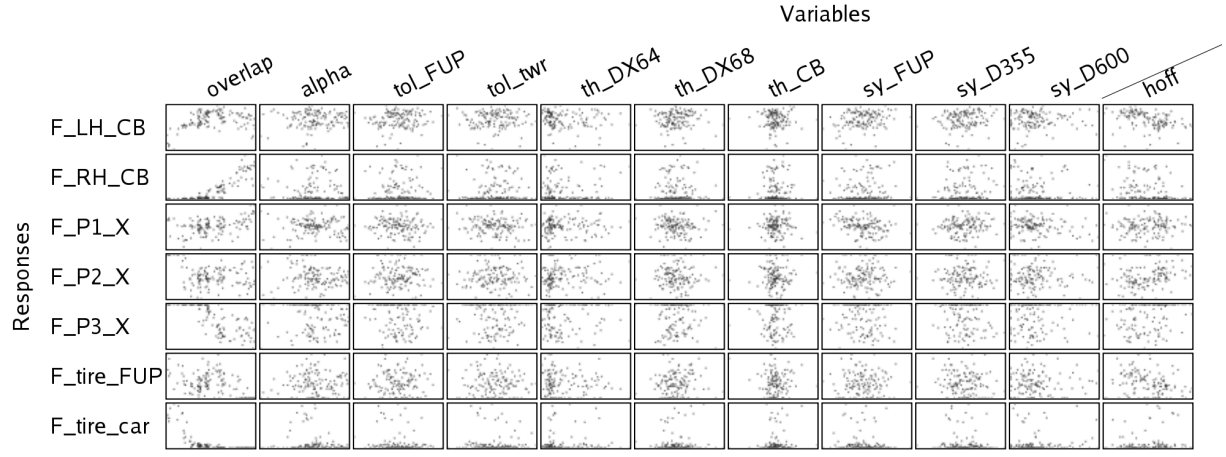

Figure A.3: Scatter plots of forces versus the input variables for the fixed energy simulation.

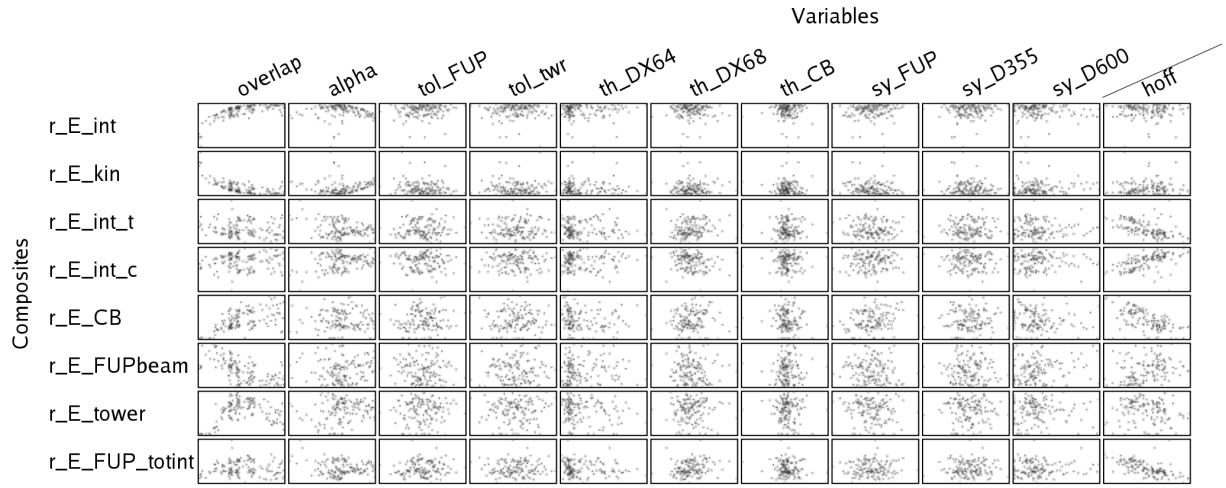

Figure A.4: Scatter plots of energy fractions versus the input variables for the fixed energy simulation.

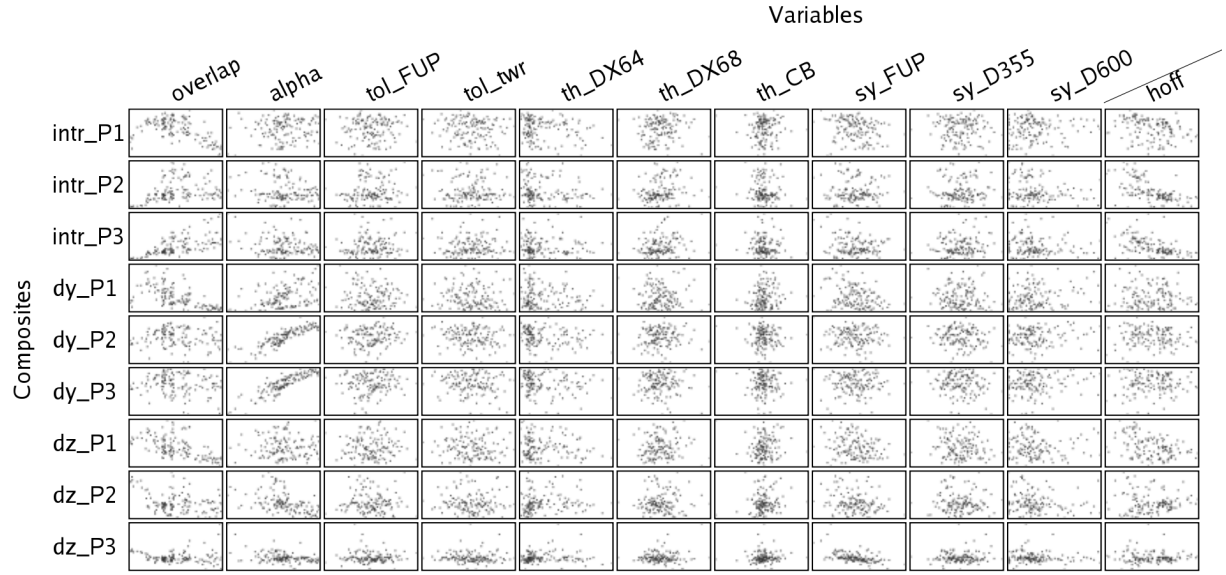

Figure A.5: Scatter plots of deformations of the truck versus the input variables for the fixed energy simulation.

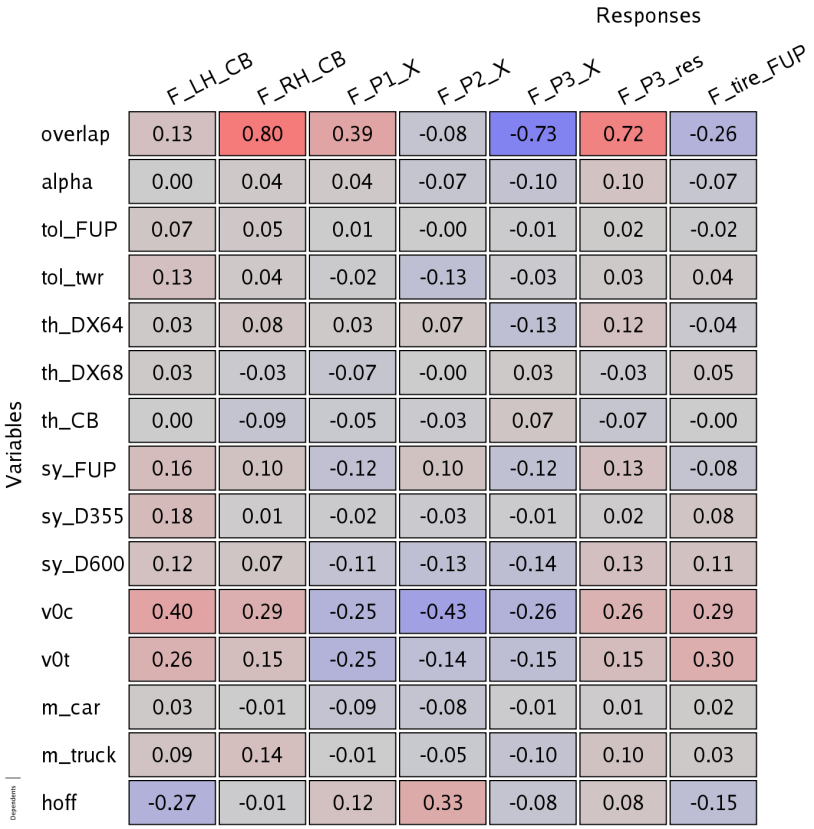

Figure A.6: Correlations of forces versus the input variables for the free energy simulation.

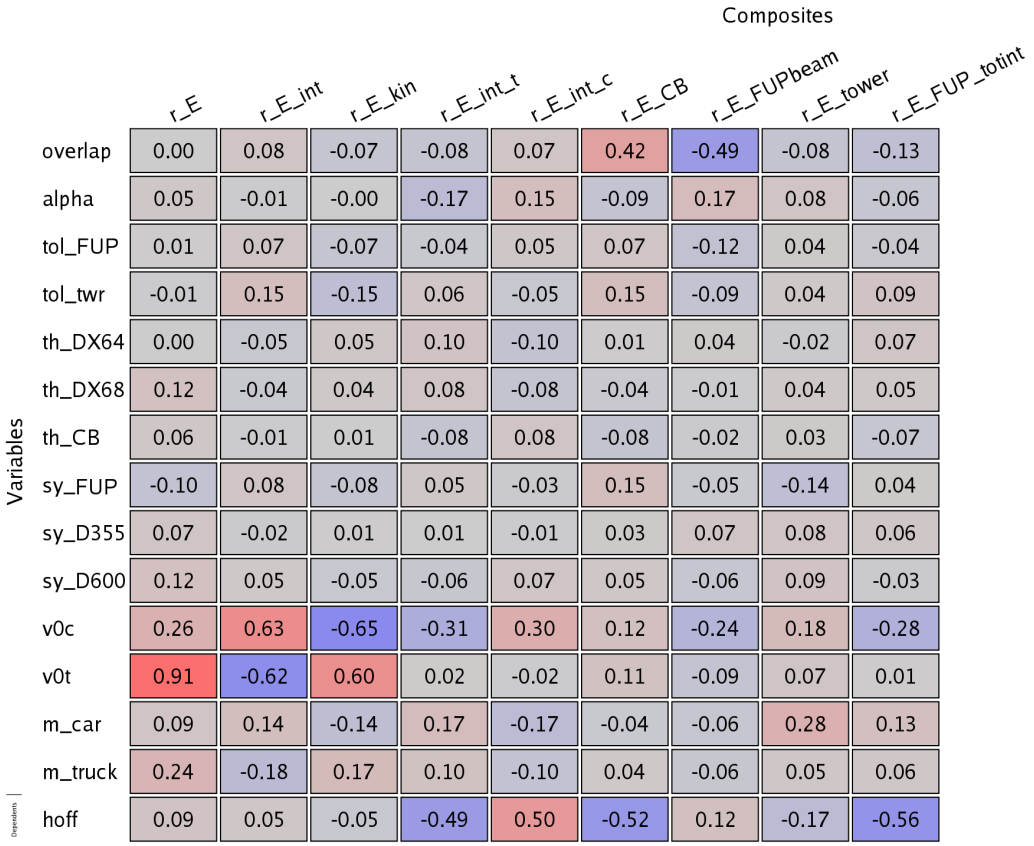

Figure A.7: Correlations of energy fractions versus the input variables for the free energy simulation.

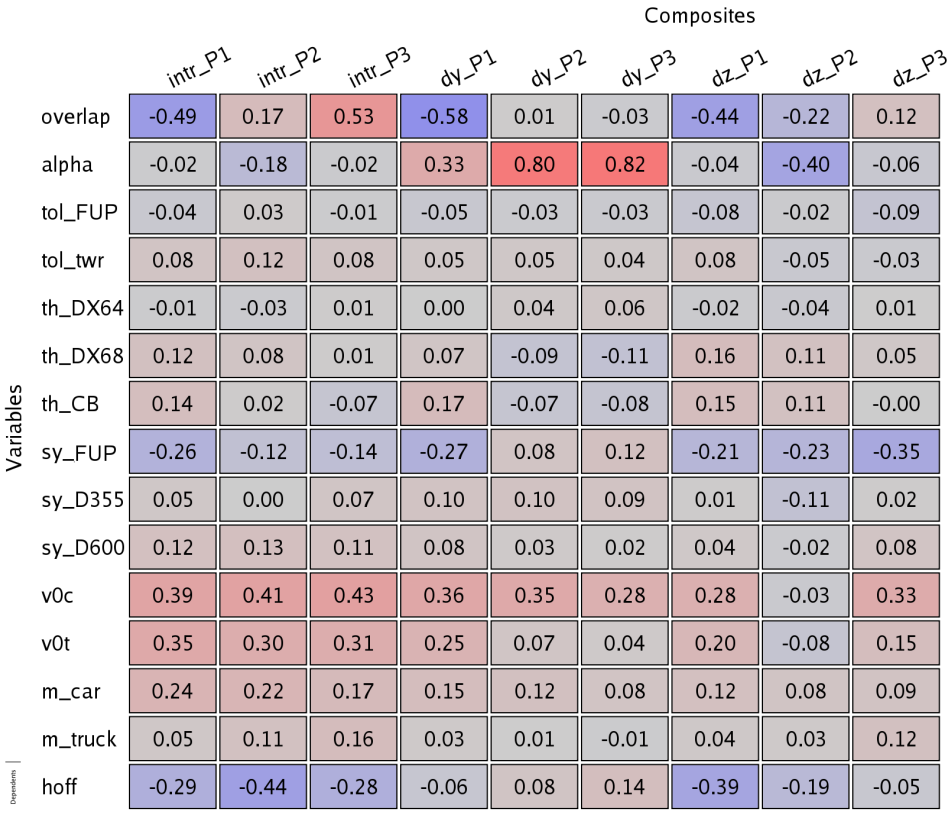

Figure A.8: Correlations of intrusions in the truck versus the input variables for the free energy simulation.